Skin contact interactions and neural encoding mechanisms underlying social and affective touch

A dissertation presented to

the faculty of the School of Engineering and Applied Science

University of Virginia

In partial fulfillment

of the requirements for the degree of

Doctor of Philosophy in Systems Engineering

by

Steven Hauser

August, 2019

Abstract

Our sense of touch provides an intuitive means of expressing social and emotional sentiment. For example, one might shake the hand of a coworker to show gratitude, or stroke the arm of a romantic partner to express love. When a "toucher" expresses a sentiment by using their hands to physically contact the forearm of a touch "receiver," populations of thousands of sensory neural afferents in the skin of the receiver respond to this contact in a way that encodes the emotion. However, several steps in this pathway are not yet well understood. In prior efforts, the contact interactions that underlie social touch—i.e., how quickly someone moves their hands, or how they stretch the skin of the touch recipient—have been studied in only a qualitative fashion. Moreover, although certain sensory afferent types are thought to be involved in social touch—such as C-tactile afferents which respond to light, stroking touch—it is not yet clear how these afferents work alongside other mechanosensitive and muscle spindle afferents in encoding emotional percepts. In this work, our goal was to determine how social touch gestures are represented at the outermost level of tactile perception—or, more specifically, how physical contact resulting from emotive human touches might evoke a peripheral response. Towards this end, we employed methods such as motion tracking, psychophysics, and microneurography. First, we ran human-subjects experiments to determine how people naturally perform a set of 6 touch expressions, by employing external motion tracking systems to measure skin-to-skin contact "primitives" such as contact area and velocity of stroking across the arm. We found that the people were naturally good at expressing the touch expressions, with high recognition rates. We also noted several different strategies used to express each emotional word (between 2 and 5), with some being more immediately recognizable. Next, we developed algorithms to measure physical contact in microneurography experiments with simultaneous neural recordings, finding differences in the responses to C-tactile and fast-adapting type II (FA-II) afferents to basic touch gestures. Finally, we measured how a set of A-beta and C-tactile afferents

responded to this measured physical contact via microneurography and motion tracking experiments performed with collaborators at Linköping University. We found that the six touch expressions could be differentiated by the firing patterns of a single afferent, namely a hair follicle afferent (HFA) or slowly-adapting type II afferent (SA-II), even amidst significant variability in how the touch gestures were performed. A better understanding of the social and emotional touch pathway could allow us to help those with social deficits to perform proper touch expressions, or create augmented means of communicating or recognizing them.

Contents

Abstract ... 2

Background ... 8

Figure B.1) Recognition rates of various emotions conveyed through touch. ... 9

Figure B.2) C-tactile afferents encode stroking touch at particular velocities. ... 11

Motivation and Significance ... 12

Gap in the knowledge base ... 12

Overview of aims ... 13

Figure O.1) Outline of dissertation. ... 14

Aim 1. Decipher the physical contact “primitives” that differentiate six emotive touch expressions as performed by naïve individuals. ... 18

Introduction ... 18

Methods ... 20

Fig 1.1) Hardware setup. ... 22

Fig 1.2) Measuring contact characteristics. ... 23

Fig 1.3) System validation. ... 25

Results ... 27

Fig 1.4) Distributions of contact characteristics for the raw dataset. ... 28

Fig 1.5) Comparing median contact characteristics per expression. ... 29

Fig 1.6) Common strategies for each expression. ... 30

Fig 1.7) Human expression recognition accuracy. ... 31

Discussion ... 32

Aim 2: Create equipment and algorithms to extract physical quantities of touch gestures simultaneously with microneurography recordings. 35

Introduction 35
Methods 37
Fig 2.1) Experimental setup. 38
Fig 2.2) Combining 2-D video and 3-D stereo infrared data to improve overall accuracy. 40
Fig 2.3) Measuring contact near the afferent's receptive field along with elicited neural spikes. 42
Results 44
Fig 2.4) Example physical contact data for each of the four gestures. 45
Fig 2.5) Responses of neural afferents to the physical quantities of human touch. 46
Fig 2.6) Peak firing rates per gesture. 47
Discussion 48
Acknowledgment 49

Aim 3: Determine how systems of Aβ and C-tactile afferents encode touch expressions and their underlying component gestures. 50

Introduction 50
Results 52
Figure 3.1) The 6 touch expressions and their physical gestures classified into components of "tapping," "patting," "stroking," or "holding." 53
Figure 3.2) Differentiability of touch expressions via single-unit responses. 54
Figure 3.3) Neural firing features which distinguish the expressions for each afferent type. 55
Figure 3.5) HFA and SA-II afferents have consistent firing patterns for the component gestures, amidst significant variability in the physical contact primitives. 58
Figure 3.6) Firing patterns of the HFA and SA-II are able to differentiate each component gesture. 59

Figure 3.7) Peak firing rate of C-tactile afferents relates to the perceived pleasantness of each touch expression. 60

Discussion 60
Methods 64
Overall conclusions and future work 69

Figure 4.1) Probability coefficients for logistic regression on physical parameters to spiking probability in 10-millisecond bins. 70

Figure 4.2) Large receptive area of HFA and SA-II, along with their sensitivity to shear, makes their responses differentiable. 71

Figure 4.3 A population model of SA-I, C-tactile, and muscle spindle afferents in the forearm for a “calming” stroke. The linear model consists of thousands of afferents, with only 1% shown in the diagram. 72

Figure 4.4 A population response to “calming” 73

Contributions 75

C.1 Diagram of my niche in naturalistic/tracked experiments. 75

Methodological Contributions 76
C.2 Ink-based method to measure contact area 76

C.3 Force-control circuitry for nonlinear elastic interactions between finger pad and compliant stimulus 77

C.4 Stereo imaging technique to measure 3-d deformation of the finger pad surface 78

C.5 Optical and electromagnetic measurement system to quantify skin-to-skin contact in human-to-human touch 79

C.6 Optical system for simultaneous measurement of neural responses and skin-to-skin contact 79

Main Scientific Contributions..80
Publications...81

References 84

Background

Human-to-human social touch. Hertenstein and Keltner were some of the first to examine social and emotional touch between pairs of people [1], [2]. In their first efforts, they considered three groups of emotions: "Ekman's emotions," such as anger, fear, and happiness; "self-focused emotions" of embarrassment, envy, and pride, as well as "prosocial emotions" of love, gratitude, and sympathy. After asking pairs of participants to convey these emotions through touch, and having the touch receiver guess which emotion was being conveyed, qualitative analysis was performed to break each emotion down into its most component "tactile behaviors"—e.g., stroking, squeezing, and shaking—as well as the duration and intensity (related to force) of each expression. They found that accuracy of recognizing the expressions ranged from 48% to 83%, demonstrating that all of the emotions were well conveyed through touch, as well as finding key differences in how the expressions were performed [1]. In subsequent efforts, a greater variety of tactile behaviors were considered, including the location of where touches were performed on the receiver's body as well as gender differences [2]. Another group examined cultural differences and participant pairs with different emotional bonds, finding that higher emotional bonds and certain cultures afforded more areas of the body responding pleasantly to touch [3]. These studies form a valuable foundation for studying social touch, but the lack of quantitative measurement makes it difficult to connect these expressions to peripheral nervous system responses. For instance, what specifically distinguishes a "tap" from a "poke," and how might these differentially activate muscle-spindle fibers, which respond only to large forces?

Table 1
Percentage of Decoding Accuracy for All Emotions

Emotion	Encoder–decoder group: Male–male	Male–female	Female–female	Female–male	Average
Well-studied emotions					
Anger	80**	77**	75**	83**	78**
Fear	60**	58**	48**	67**	56**
Happiness	44*	61**	59**	75**	60**
Sadness	44*	52**	57**	42*	50**
Disgust	48**	48**	43**	67**	50**
Prosocial emotions					
Love	64**	71**	61**	79**	68**
Gratitude	76**	77**	70**	75**	74**
Sympathy	64**	65**	70**	67**	67**

* $p < .05$. ** $p < .01$.

Figure B.1) Recognition rates of various emotions conveyed through touch. From Hertenstein and Keltner 2009 [2]. The touch expressions in these experiments were almost completely unrestricted in terms of what gestures to perform and where to make contact on the receiver's body, and had high recognition rates.

Microneurography. Microneurography is a long-standing procedure for measuring single-unit responses of peripheral neurons in awake, conscious humans [4]. It is used to measure both motor control neurons, such as in the diagnosis of some pathologies, as well as measuring sensory responses. The technique requires a skilled researcher to insert a microelectrode (usually tungsten, 1-5 microns in diameter at the tip) into a large nerve, and circuitry to amplify its impulses electronically. The technique does not cause pain and therefore does not require sedation or anesthesia. With the electrode inserted, trains of action potentials (rapid changes in cell membrane potential) in the nerve can be recorded and analyzed. Due to the conduction velocities of some nerves, especially unmyelinated afferents such as the C-tactile afferents, delay in the conduction of these potentials down the arm must be considered when examining the results.

Neural encoding of social touch. There are thousands of afferents of various types in the skin, with distinct densities and response properties; for example, some respond to heat or cold, some respond to vibration, and some respond to movement of hairs on the skin. Among these afferents, there are several subtypes are likely to be involved in encoding social touch information. A-beta fibers are myelinated afferents discovered over a hundred years ago, and have three main subtypes relevant to social touch: SAI afferents, which are known for encoding fine spatial detail related to stress distributions within the skin, SAII afferents, which respond to stretching of the skin, and RA afferents, which respond to the onset and offset of stimulation. Another class of afferents, C-tactile fibers, were discovered much more recently, and are possibly the most intriguing type with respect to social touch [5]. These afferents project to the insular cortex, close to where emotional processing occurs, and are unmyelinated, thus slower and evolutionarily older. C-tactile afferents respond maximally to light, stroking touches at specific velocities [6], in the range of human body temperature [7], and additionally are associated with pleasant or hedonic sensations [8]. For this reason, many attempts to create mechanical stimulation replicating social touch have focused on stimulating C-tactile afferents [9]. Finally, although not typically associated with sensation, muscle spindle fibers have been found to respond to high-force expressions that might be associated with poking or tapping. So far, studies aiming to characterize these afferents have employed tightly controlled, mechanical stimuli [5], [10]; to further explore their role in social touch, it is imperative to study their responses to naturalistic stimulation from a human hand.

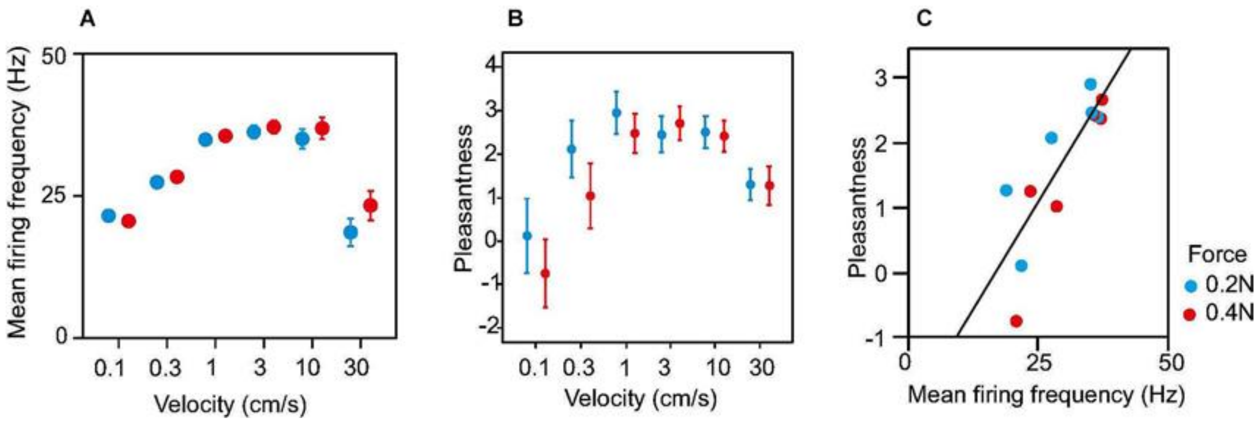

Figure B.2) C-tactile afferents encode stroking touch at particular velocities. From Loken et al., 2009 [8]. A) shows the specificity of CTs for 1-10 cm/s stroking, and a correlation with pleasantness (C).

Human-to-robot social touch. In addition to studies of human-to-human touch, prior efforts have worked on training robots (typically humanoid or zoomorphic) with sensor arrays to recognize different kinds of tactile behaviors, such as poking, tapping, and stroking [11]–[15]. Unlike the human-to-human studies, these experiments have allowed for measurement of physical quantities such as contact area and contact force, as well as determining how people naturally interact with robotic animals or sensor pads. Often the end goal of such works is to train a machine learning algorithm to recognize the expressions, which has been generally successful [11]. These experiments demonstrate that there are in fact quantitative differences between social touch expressions; as such, there is likely utility in performing such measurements to study human-to-human touch as well.

Motivation and Significance

Social touch is an important part of our everyday interactions with others and provides an intuitive and personal means of conveying information. This work seeks to better understand the physical and neural basis of social touch. One application of these results is in building devices to artificially stimulate the skin, which might be used for remote or augmented social touch communication. Another application is in social robotics, designing robots that can interpret human social touch for use in communication or therapy. Finally, such information can be used to help those with social deficits, in instructing them how to properly perform or interpret social touch gestures.

Gap in the knowledge base

Our current understanding of how physical touch is able to communicate social or emotional information is very limited. At a qualitative level, we know that to convey specific emotions, humans generally use certain hand movements (i.e., poking or squeezing) on certain parts of the receiver's body (i.e., the arm or the shoulder) [1], [2]. These hand movements press into the receiver's skin and muscle, stimulating diverse and numerous populations of sensory neural afferents, such as C-tactile fibers and muscle spindles. However, exactly which of these afferents are important, and how their firing properties might differentiate human touches, is unknown. This brings us to a research question: how do the physical quantities related to human-to-human social touch evoke sensory afferents to form an emotional percept? Our **central hypothesis** is as follows: Amidst superficial variability in how individuals perform a set of emotional touch gestures, underlying physical contact interactions at the level of skin and tissues can distinguish them. Together, five classes of sensory afferents encode these social ideas through distinct patterns of spatial and temporal firing.

Overview of aims

Our sense of touch provides an intuitive means of expressing social and emotional sentiment. For example, one might shake the hand of a coworker to show gratitude, or stroke the arm of a romantic partner to express love. However, little is understood about how a person naturally performs such expressions; i.e., what is the speed with which the hand moves, or what patterns of force are applied? Likewise, we do not understand how physical contact with the recipient stimulates sensory afferents in their skin, and how this triggers an emotional response. The work proposed herein seeks to address these gaps by 1) measuring and characterizing the physical contact resulting from naturalistic social touch expressions between people, and 2) measuring how such physical contact elicits and encodes responses from neural afferents in the skin. Ultimately, we seek to decipher precise contact interaction cues that readily communicate a set of common emotive words. A better understanding of how touch expressions are performed and encoded is critical in building haptic devices for remote or augmented social touch communication, or in helping those with social deficits learn to properly perform or interpret social touch expressions.

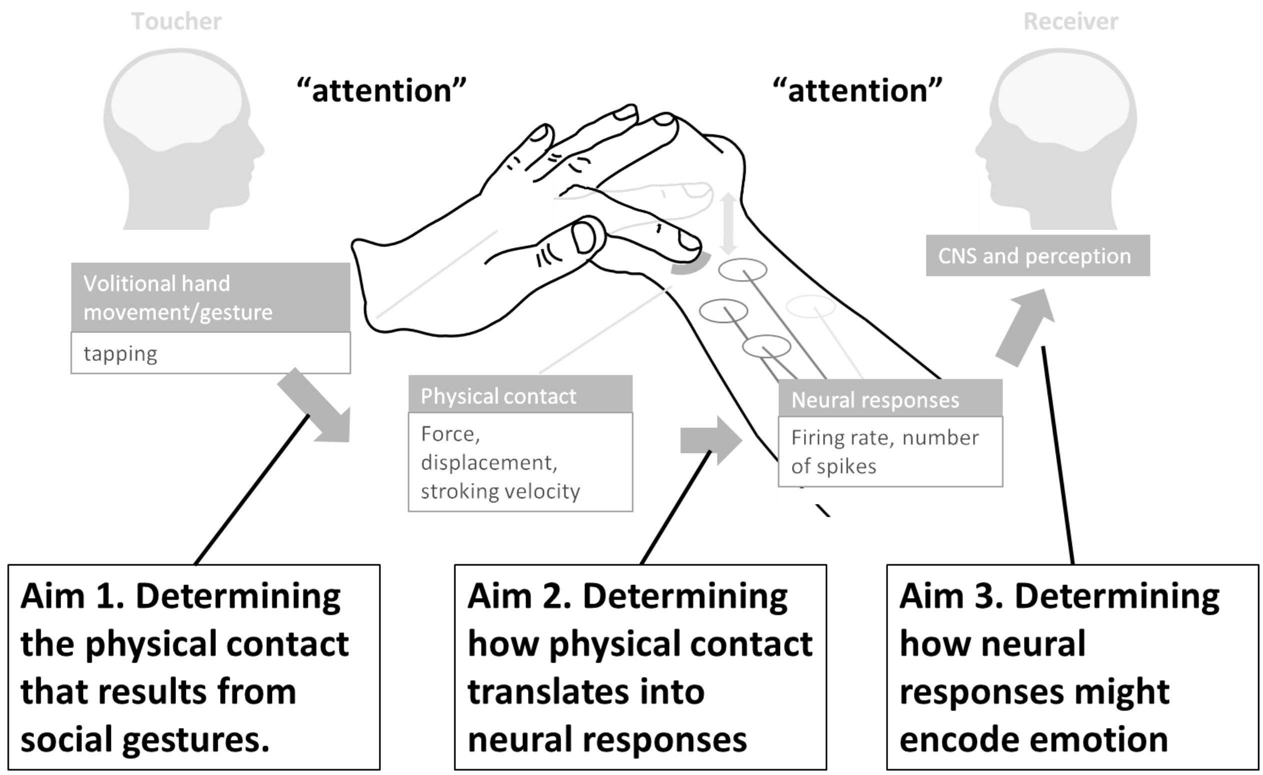

Figure O.1) Outline of dissertation. Aim 1 is concerned with the translation of social touch gestures, i.e., "calming" and "attention" into physical quantities such as "displacement" and "stroking velocity." Aim 2 focuses on then determining how these resultant physical quantities stimulate neural responses. Finally, Aim 3 attempts to examine how a set of peripheral afferents can encode these quantities differentially.

Aim 1: Decipher the physical contact "primitives" that differentiate six emotive touch expressions as performed by naïve individuals.

Although studies on human-to-robot touch have quantified physical contact interactions underlying social expressions through the use of sensor mats—i.e., contact area, pressure, etc.—the study of human-to-human touch thus far has been based on qualitative observation. We addressed this gap with a set of lightly constrained human-to-human touch experiments in which we employed external tracking systems to quantify skin-to-skin contact. Psychophysical experiments were conducted with ten pairs of romantic couples, in which one participant was asked to touch their partner's forearm and attempt to convey one of six emotional words. During the experiments, behavioral data was collected using motion tracking equipment, which consisted of a stereo infrared camera system to measure the movement of the toucher's hands and an electromagnetic tracking system to measure the position of the touch recipient's forearm. The resultant data was analyzed to determine physical contact "primitives" per each touch expression such as position on the arm, total contact area, tangential and normal velocities relative to the arm, and mean duration of contact. As an end result, we constructed a system for the measurement of these physical primitives, and gleaned a general idea of how each of the six expressions are performed naturally by naïve participants. We further identified component expressions associated with each expression that were most readily recognizable and intuitive.

Aim 2: Create equipment and algorithms to extract physical quantities of touch gestures simultaneously with microneurography recordings.

Traditionally, the characterization of neural afferents relies on the use of carefully controlled, mechanical stimuli; however, to study human-to-human touch, we need to understand how sensory afferents of the forearm respond to naturalistic, and therefore less controlled, touches of the human hand. In a set of microneurography and behavioral experiments conducted with collaborators at Linköping University, we measured neuronal firing simultaneously with physical contact primitives (as in Aim 1) as "expert touchers" performed basic touch gestures on the receptive field of single fibers. Here we used a new tracking methodology combining 3-D hand tracking (via Leap Motion) with 2-D finger tip tracking in HD video, along with a basic contact model similar to that in Aim 1. Afterwards, we determined basic relationships between our contact primitives and the output firing frequency of two types of afferents: a C-tactile afferent and an FA-II (Pacinian) afferent. We found the C-tactile afferent to respond at high frequency to stroking gestures, while the FA-II was able to respond synchronously to tapping gestures. The results indicated that this method holds promise in determining the roles of unique afferent types in encoding social and emotional touch attributes in their naturalistic delivery.

Aim 3: Determine how systems of Aβ and C-tactile afferents encode touch expressions and their underlying component gestures.

Our final aim was to investigate the neural encoding of social touch expressions. One primary goal was to determine which afferent subtypes are most likely to be involved in human touch. A secondary goal was to investigate at which level in the nervous system might human touches expressions be differentiated (i.e., single units, spinal cord, or the brain). In novel human-to-human touch microneurography experiments, we investigated the neural responses of single unit neural afferents to our six touch expressions. The motion tracking system from Aim 2 was used to further quantify and characterize the touches along with the neural recordings which were performed by Linköping University. Via machine learning and statistical methods, we found that particular subtypes of neural afferents (namely, the HFA and SA-II afferents) were capable of encoding the touch expressions via responses of just a single unit.

Through further study, we determined that this was due in part to their robust encoding of the component gestures of each expression, i.e., tapping, patting, holding, and stroking. When further looking at the perceived pleasantness of the six expressions, we found a positive correlation with the C-tactile response, confirming 1) that it is activated well by human touch stimuli and 2) that it seems to be signaling pleasant, innocuous touch, as previously hypothesized. Further study is required to place these responses in a population-level context, but it seems that the mechanisms may be in place to decode emotive touch expressions via a single first-order neuron. Indeed, human affective touch gestures may be encoded very distally in the periphery.

Aim 1. Decipher the physical contact “primitives” that differentiate six emotive touch expressions as performed by naïve individuals.

Abstract—Couples often communicate their emotions, e.g., love or sadness, through physical expressions of touch. Prior efforts have used visual observation to distinguish emotional touch communications by certain expressions tied to one’s hand contact, velocity and position. The work herein describes an automated approach to eliciting the essential features of these expressions. First, a tracking system records the timing and location of contact interactions in 3-D between a toucher’s hand and a receiver’s forearm. Second, data post-processing algorithms extract dependent measures, derived from prior visual observation, tied to the intensity and velocity of the toucher’s hand, as well as areas, durations and parts of the hand in contact. Third, behavioral data were obtained from five couples who sought to convey a variety of emotional word cues. We found that certain combinations of six dependent measures well distinguish the touch communications. For example, a typical sadness expression invokes more contact, evolves more slowly, and impresses less deeply into the forearm than a typical attention expression. Furthermore, cluster analysis indicates 2-5 distinct expression strategies are common per word being communicated. Specifying the essential features of touch communications can guide haptic devices in reproducing naturalistic interactions.

Introduction

Touch is an effective medium for conveying emotion, such as expressing gratitude to a friend or comforting a grieving relative. Indeed, naturalistic expressions of emotion are a part of daily life and fundamental to human development, communication, and survival [16]. Unraveling how our nervous system encodes emotion is an emerging topic. Recent works indicate that emotion is encoded, at least in part, by unmyelinated C tactile (CT) afferents that project to the insular cortex [17]. This pathway is distinct from, yet somewhat redundant with, that of discriminative touch whereby low-threshold mechanosensitive afferents convey information to the somatosensory cortex. On-going endeavors are attempting to understand relationships between stimulus inputs and sensory percepts, at levels of single-unit microneurography, cortical fMRI, and behavioral psychophysics [6], [18], [19].

We currently know little about the rich, naturalistic details that underlie what is communicated in human-to-human touch, whereby individuals convey emotions through unrestricted, intuitive touch. It is thought that certain contact interactions underlie how one seeks to convey an emotional message such as love or gratitude [1], [2]. In this setting, the stimulus is often found at the physical contact of the toucher's hand with the receiver's forearm. Indeed, qualitative observation has told us of the importance of hand intensity, velocity and position. In particular, Hertenstein and Keltner examined "Ekman's emotions," of anger, fear and happiness, "self-focused emotions" of embarrassment, envy, and pride, as well as "prosocial emotions" of love, gratitude, and sympathy. Each emotion was broken down into its most component tactile behaviors – e.g., stroking, squeezing, and shaking – as well as the duration and intensity of each expression. They found that accuracy of recognizing the expressions ranged from 48% to 83%, demonstrating the emotions were well conveyed through touch, and finding key differences in how the expressions were performed.

While the study of emotional expressions has mostly been limited to qualitative observation, other works have begun to quantify and classify expressions using, for example, pressure data derived from touch-sensitive surfaces [11]. From an engineering perspective, such efforts can help identify and quantify the essential features underlying the interactions – amidst very rich yet variable physical contact – so as to replicate these emotions with haptic actuators [9], [20]. Quantitative descriptions may also help more precisely understand how such interactions are encoded by the nervous system. For example, CT afferents respond maximally to velocities from about 1 to 10 cm/s [8] and A-beta afferents to both indentation and velocity [21]. Thus, a system to characterize details underlying these expressions – e.g., contact area, velocity, and position – is necessary to better understand the communication of affective touch. However, the use of pressure mats, in particular, can be problematic in that they can change the psychological and physical nature of how one person delivers the expressions to another, and attenuate their response. In particular, mechanosensitive afferents respond to forces at 0.08 mN (i.e., less than the weight of such a mat), to light shear force at the skin's surface, and human body temperature [7], [22].

Towards the goal of quantifying emotional expressions, this work describes the customization, combination and validation of infrared video and electromagnetic tracking systems to measure contact between a toucher's hand and a receiver's forearm. In human-subjects experiments, we examine how these metrics differ when the toucher is asked to convey distinct sets of emotionally-charged words. The overall goal is to identify "primitive" attributes that underlie these contact metrics and tie those with the most salient perceptual responses.

Methods

By analyzing hand and forearm movements with a motion tracking system, we 1) quantify how romantic couples touch one another when attempting to convey a variety of emotions, and 2) determine which characteristics of the contact interaction might encode each emotion. First, we built a tracking system to measure the "toucher's" hand (who performed the expression) and the "receiver's" forearm (who responded to the expression). We then conducted behavioral experiments with five romantic couples, in which one participant attempted to convey one of six words to the other using only touch, "attention", "calming", "gratitude", "happiness", "love", and "sadness." Four of these words were chosen as a representative subset from prior work [2], with "happiness" and "sadness" as two of "Ekman's emotions," and "love" and "gratitude" as two prosocial emotions. We also chose two other words, "attention" and “calming.” The participants were naïve to the task such that they would perform intuitive, naturalistic expressions. In post-processing the data, we sought to identify contact characteristics underlying expressions used to convey each emotion. We further broke down each expression into subgroups of expression strategies.

Behavioral experiments. Behavioral experiments with human subjects were performed as approved by the Institutional Review Board. In particular, five male-female romantic couples were enrolled, for a total of ten participants (mean age = 23.8 years, SD = 1.7, all right-handed) from the east coast of the United States of America. Each couple had been together at least three months (mean duration = 1.7 years). All enrollees granted consent to participate and continued to completion.

The couples were asked to perform expressions conveying one of six emotions to one another: “attention,” “happiness,” “calming,” “love,” “gratitude,” or “sadness.” Before each experiment for approximately five minutes, the touchers and receivers individually were given the list of the six words and asked to think about how they might perform expressions for each emotion. During each experiment, one participant of the couple would be chosen randomly to first be either the “toucher” or the “receiver.” Afterwards, the couple would switch roles, such that each one would act as the “toucher” and the “receiver” once. Both toucher and receiver were seated and separated by a curtain, such that the toucher could see the receiver’s forearm, as it rested on the armrest of a chair, with no other visual contact.

The receiver was given a laptop computer, which was used to record an individual response and queue the next question to the toucher, while the toucher was given a set of headphones over which the next emotion word was stated. For each trial, the toucher was instructed through the headphones to convey one of the six words to the receiver. The toucher was asked to touch only the forearm of the receiver, and to continue to perform the touch expression for a full ten seconds, until instructed to stop through the headphones. Afterwards, the receiver was given seven seconds to choose which on-screen word they thought the toucher was trying to convey. Each of the six words was repeated five times during each experiment for a total of thirty expressions per participant. The tracking system was used over this duration to continuously measure the relative motions of the receiver's hand and toucher's forearm.

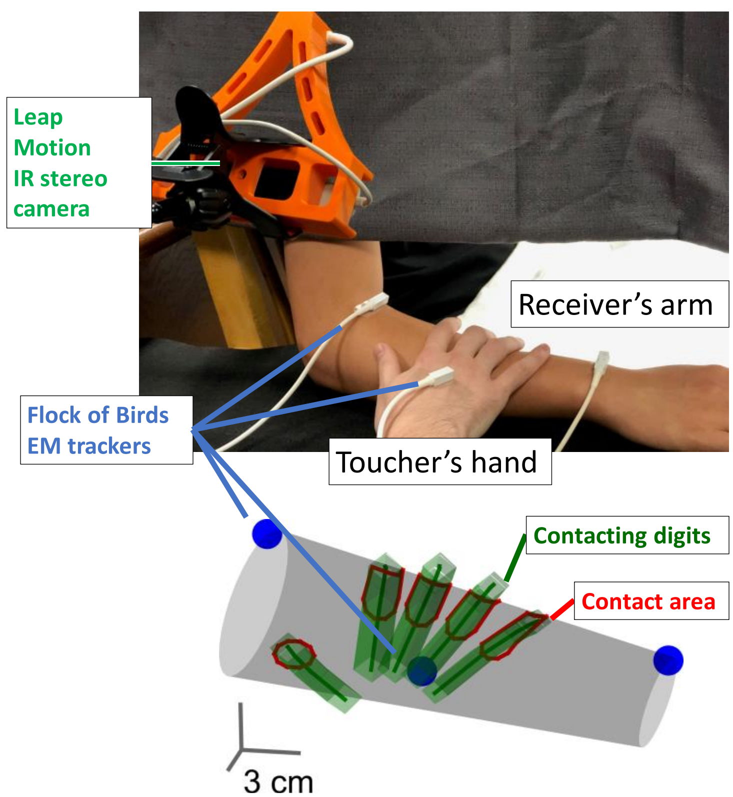

Fig 1.1) Hardware setup. (Top) Contact between the toucher's hand and receiver's forearm was measured using motion tracking equipment, consisting of a stereo infrared camera device to measure the toucher's hand and an electromagnetic tracking system to measure the receiver's arm, as well as orient the toucher's hand. (Bottom) A virtual representation of the hand and forearm illustrate the data captured along with the measured contact between them.

Tracking system. We customized off-the-shelf equipment to track a toucher's hands in contact with a receiver's forearm (Figure 1.1), consisting of electromagnetic tracking devices (Trakstar and Model 800 sensors, Ascension, Shelburne, VT) and infrared cameras and LEDs (Leap Motion, San Francisco, CA). These simultaneously enabled high accuracy while minimizing the physical attachment of the tracking equipment to the participants. Data were collected at approximately 30 Hz. To measure and track the forearm of the receiver, two Flock of Birds sensors were attached to the dorsal side of the forearm via double-sided tape, at the wrist and elbow. Each sensor tracked six dimensions of translation and rotation to an accuracy of 10 microns. The circumference at both locations was measured via tape measure. A 3-D conic section was fit to these measurements to represent the virtual forearm.

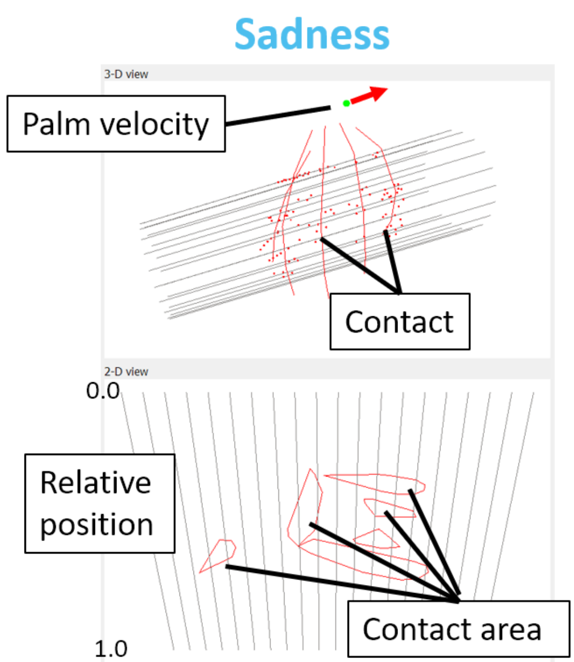

Fig 1.2) Measuring contact characteristics. Screenshots of the custom-built tracking software demonstrating some of the contact metrics at a single time point as the toucher conveyed "sadness." (Top) A series of lines form a cylinder representing the forearm of the receiver, and other lines crossing those represent the fingers and digits of the toucher's hand. Red dots are intersections between the two delineate contact being made. (Bottom) The same forearm of the receiver is represented, but this time the series of lines is unwrapped onto a flat 2-D surface. Red areas denote contact.

To measure and track the hand of the toucher, the Leap Motion controller was used in conjunction with one Flock of Birds sensor. The controller was mounted onto a 3-D printed housing, with the Flock of Birds sensor at a distance of 10 cm to avoid electrical noise from the Leap Motion controller. By fixing the position of this sensor and the Leap Motion controller together, hand coordinates could be transformed using the sensor pose into the same reference frame as the forearm coordinates. An additional Flock of Birds sensor was securely taped to the back of the toucher's dominant hand for increased precision – the hand position was relocated based on this sensor position if it did not match properly in the recording.

Extracting contact characteristics. Data from the Leap Motion controller resulted in poses, widths and lengths for each bone of the hand. In custom-built software, these were translated into cylinders made up of 3-D line segments. Each intersection between a line segment and the forearm cone was treated as a contact point (Figure 1.2).

Contact characteristics. We examined six contact characteristics for each expression, which were captured at each recording frame of the tracking system. All values were only considered when contact was made between toucher and receiver. For example, if the hand was picked up from the arm and moved rapidly to another point on the arm, this velocity would not be included in the calculations. The six contact characteristics were as follows. 1) Normal velocity was measured by the forward divided difference to the next measured position for palm or finger tips in contact with the arm, projected onto the surface normal of the closest point on the arm. This quantity related to the indentation-rate of each expression; i.e., we found that expressions with high normal velocity tended to also have high force, but the measurement of normal velocity was more robust from a noise perceptive. 2) Tangential velocity was measured by the forward divided difference to the next measured position of the palm, projected onto the plane tangent to the closest point on the arm (orthogonal to the surface normal). 3) Contact area was determined by the area of the convex hull enveloping the contact points for each bone in the hands (as is illustrated in Figure 1.2). 4) Mean duration of contact was measured as the mean continuous duration of contact made with the arm during a expression. 5) The number of fingers contacting was determined by averaging the sum of binary “in contact” values per finger over the expression. 6) The time with palm in contact was measured as the proportion of time in which the palm was in contact with the arm out of the total contact time.

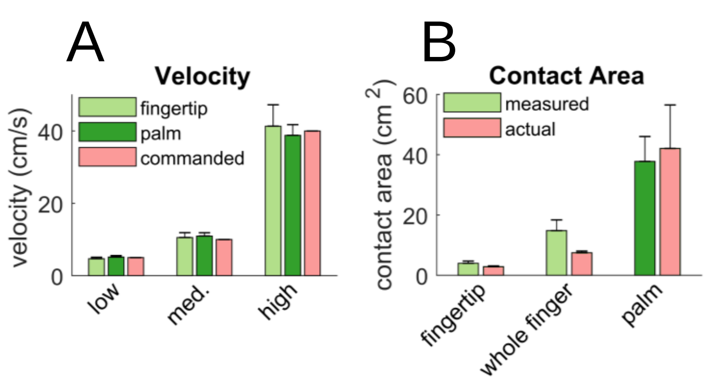

Fig 1.3) System validation. Tests of the hardware setup were conducted to evaluate the means of estimating the: A) velocity of index fingertip and palm, B) contact area. Contact area was compared to actual measurements using an ink-based technique [23], [24]s.

System validation. An experiment was performed with a single participant to examine the accuracy of the tracking system in measuring velocity and contact area (Figure 1.3). To command velocity, two marks were made on the receiver's arm 4 cm apart, and the toucher moved their palm (or fingertip) between the marks according to a metronome commanding the desired velocity. To measure contact area, the toucher's hand was covered in washable ink and pressed against the receiver's forearm [23]. Ink prints were later compared to output from the tracking system.

Data analysis and statistics. The final cleaned dataset consisted of 227 of the 300 performed expressions, as some expressions were not properly recorded due to inconsistencies in the Leap Motion's output [25]. A research assistant viewed each the motion tracking recording to remove any cases where the hand position was erratic or not picked up at all. In post-processing, only the toucher's right hand was considered to simplify the comparisons across expressions (or the left hand if the right hand was not used). For each expression, the six contact characteristics were averaged for all frames in the expression, given contact was made in that frame.

Next, statistics were performed on the raw dataset (scikit-posthoc library and Scipy statistics packages, Python 2.7) using a conservative, non-parametric approach. A Kruskal-Wallis test was performed for each of the six contact characteristics across the expressions to determine significant differences. Afterwards, a post-hoc Conover's test was performed to identify differences between expressions using the Holm-Bonferroni method for p-value correction.

Finally, clustering analysis was performed to determine the most common expression strategy for each expression. Values were scaled from 0 to 1 based on the full range of values of each of the six contact characteristics. K-means clustering was performed (scikit-learn library, Python 2.7). The sum-squared errors were scored for values of k from 0 to 10 and a suitable value for k was chosen via the elbow method. Representative expressions were chosen from the dataset as those closest to the centroid of each identified cluster. Within each expression, a representative snapshot was drawn to represent the expression.

Results

Raw data for the expressions are detailed in Figure 1.4. At first glance, most of the metrics exhibit a high level of variability across the ten participants, but there were several noteworthy trends. Summarizing these trends, Figure 1.5 shows the median expression characteristics from the dataset. Attention and happiness, for example, had especially high normal velocity, suggesting that these were comparatively high force expressions. Happiness and calming were particularly high in tangential velocity, with love and sadness especially low, as often these expressions were motionless. Contact for calming, love, sadness, and happiness was usually maintained for the full duration of the trial, while gratitude, happiness and attention had noticeably shorter durations. Attention in particular stands out in terms of palm contact being rarely made, the low number of fingers in contact, and the total area of contact being low.

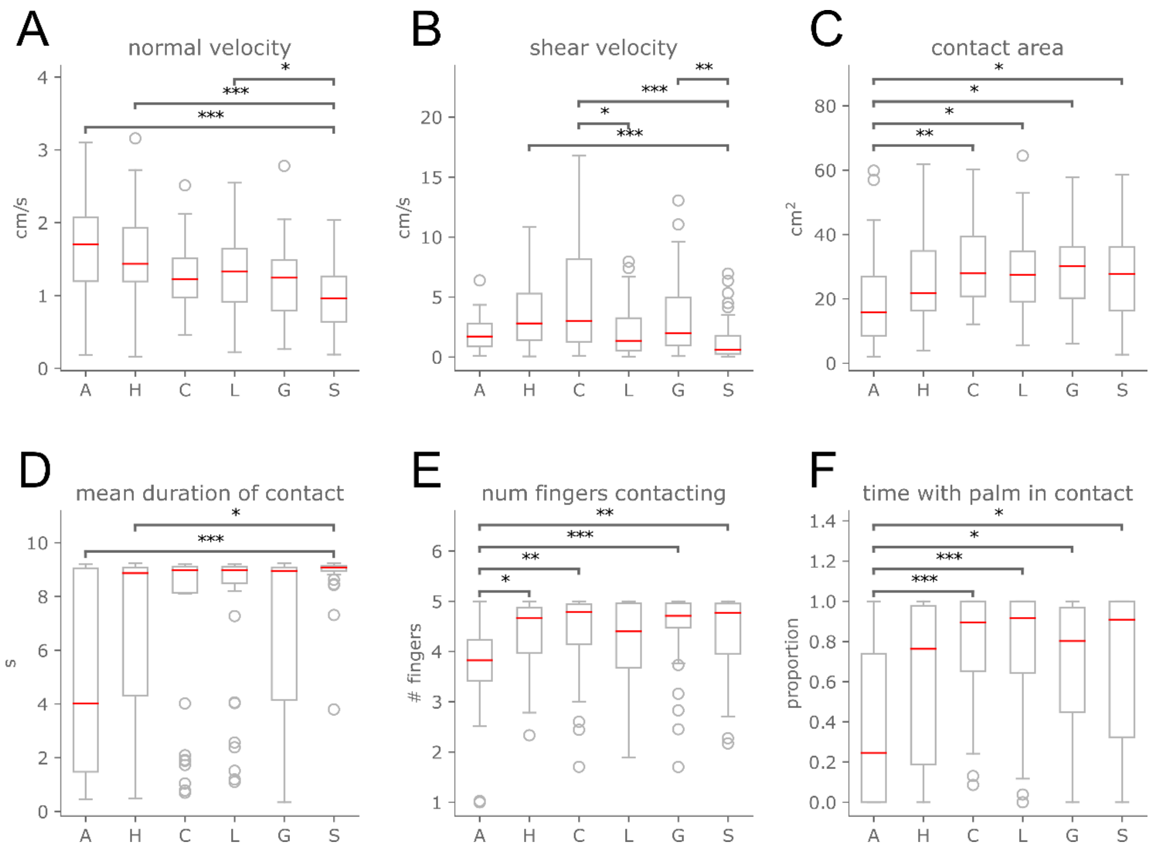

Fig 1.4) Distributions of contact characteristics for the raw dataset. All measurements were taken from the toucher's right hand. A) shows the mean velocity of contacting fingertips and palm in the direction towards the surface normal of the arm, relating to indentation-rate or intensity of the expression. B) shows the tangential velocity of the contact, or the velocity vector projected onto the tangent plane of the closest point on the arm. C) plots the total contact area for each expression, summed for the palm and fingers. D) plots the mean duration of contact made between toucher and receiver within each trial. E) depicts the mean number of fingers contacting the arm throughout each expression. F) displays the proportion of total contact time in which the palm was touching the receiver. * $p <= .05$, ** $p <= .01$, *** $p <= .001$. A = attention, H = happiness, C = calming, L = love, G = gratitude, S = sadness.

Fig 1.5) Comparing median contact characteristics per expression. Each contact characteristic is normalized based on the average IQR across each expression. Normal and tangential velocities in particular well separate the 6 expressions.

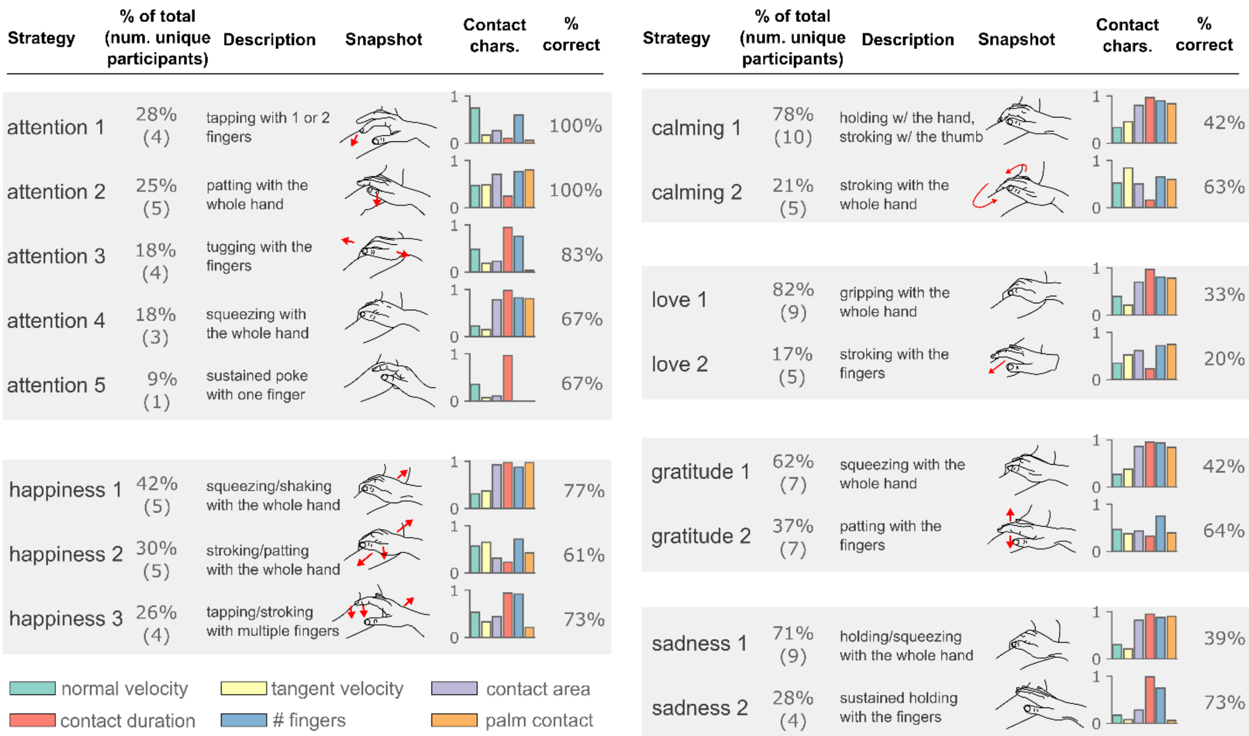

Fig 1.6) Common strategies for each expression. Via k-means clustering analysis, multiple “expression strategies” were determined. For each expression, the strategies are listed, along with 1) the percent of the expressions that were clustered into each strategy, 2) the number of unique participants which used each expression (out of 10), 3) a description along with a representative “snapshot” of each expression, 4) the relative quantities of our six contact characteristics, and 5) the percent of the time that the receiver correctly identified the strategy. % total values are floored to the nearest whole percent.

Further work was done to determine common expression strategies of each expression via clustering analysis (Figure 1.6). Attention was the most variable expression, with five strategies identified. Most common were short, high-intensity pokes with a small number of fingers. However, faster pulling on the arm with the whole hand was also seen with somewhat high frequency. A few participants used low intensity, high duration expressions to signal attention. The next most variable expression was happiness, with three primary strategies identified. Most common were whole-hand expressions, although tapping with the fingers was also fairly common. All of the happiness strategies were relatively high with respect to tangential velocity. The most consistent expressions were calming, sadness, and love, with approximately 75% of these expressions being performed in a similar manner. For calming, either a low intensity, slow hold with the hand was used or a faster stroking expression with the fingers. For gratitude, a slower grabbing motion or a faster shaking motion was used. For sadness, either a whole hand expression or holding with a few fingers was used. Notably, both sadness strategies were always held for the whole trial.

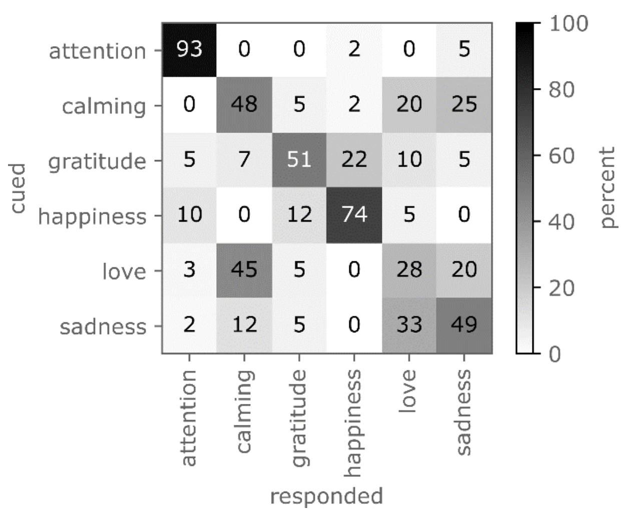

Fig 1.7) Human expression recognition accuracy. The confusion matrix from the human-subjects behavioral experiments. Overall classification accuracy was 57%.

Behavioral experiments analysis. We also examined how receivers perceived the expressions (Figure 1.7). Participants were especially accurate in recognizing “attention” and “happiness” (93% and 74% correct, respectively). The worst performance was in recognizing “love” (28% correct), which was most often misrecognized as calming (45% responded). Recognition accuracy across all six expressions was 57%.

Discussion

We frequently communicate emotion with others through touch cues. Rich spatio-temporal details underlie how a toucher’s fingers and palm make contact in interactions with a receiver’s forearm. Prior efforts have used mostly qualitative, human visual observation to distinguish an emotion by certain expressions tied to one’s hand contact, velocity and position. The work herein describes an automated approach to quantitatively eliciting the essential features of these expressions that convey an emotion’s meaning. We developed six quantitative contact characteristics that were capable of describing and differentiating the expressions used to communicate our word cues that varied in emotional content. Furthermore, clustering analysis revealed that there are typically 2-5 expression strategies per expression and that some lead to more successful communication of an emotion. Abstracting emotive touch expressions into quantitative contact characteristics, or primitives, may help in specifying design requirements to be implemented with haptic actuators.

Among our sample of ten participants, we found that certain expression strategies, i.e., combinations of the six contact characteristics, seemed to better convey certain emotions. One interesting finding came with regards to expressions of calming, love, and sadness. These expressions tended to be performed using strategies that are very similar to each other with respect to our six contact characteristics (see Figure 1.6, calming 1, love 1, and sadness 1). When touchers used those strategies, the receiver’s recognition dropped significantly, as one might expect. However, when using alternate expression strategies that varied from one another more significantly, recognition accuracy was much greater (see

Figure 1.6, calming 2, sadness 2). This suggests that our quantitative analysis captures similar features to what the receivers use in their judgments, or at least that we have avoided capturing discriminative features to which the receivers are insensitive.

Tied to this are questions of whether the expressions used are innate or are learned on the fly to solve the particular tasks of this study, and of whether one's ethnic or cultural background and norms influence one's expressions. Such questions could be the topic of further study. A larger study size is also needed to confirm the trends found herein – the uniqueness of the six contact characteristics – as our focus was to introduce a new approach to automate the tracking of features. Indeed, while the six characteristics are promising and tied to prior research, their number may need to be reduced or expanded. For one, the time duration to perform a expression was held constant but might be an important variable.

Moreover, another next step is to determine the precise ranges and timescales for each of the six contact characteristics. For instance, perhaps contact area must be 1.0 cm and not 1.5 cm, rate must be 3 cm/sec, delay between subsequent touches 100 ms not 300 ms, etc. With the setup described herein, it is possible to investigate such questions. Some of their ranges may relate to receptive field size and density organization, integration of mechanosensitive afferent responses, as well as other perceptual mechanisms.

At a deeper level, deciphering the specific input-output relationships that tie contact on the forearm to populations of neural afferents in the skin (and further on to perception) is critical to our understanding of how these emotions are encoded [26]. The engagement of the CT afferents is particularly interesting, as these are associated with pleasant or hedonic touch [8] – in fact, we do note similarities in the range of tangential velocity of our expressions to the maximal activation range of these afferents (1-10 cm/s).

More broadly, a better understanding of these input-output relationships can greatly assist in generating design requirements for tactile communication devices and sensory prosthetics. Ideal devices should evoke the same behavioral responses as real human touch, although a device that falls short of this ideal may still be successful if it engages physiological systems sufficiently well. Some groups have worked to create such devices capable of creating stroking sensations on the arm [9], [20] which could be used for such a purpose. Measurements from our system should serve as a basis for the design specifications of these devices, providing critical information such as the contact areas and indentation velocities that need to be replicated.

Finally, in addition to machine-to-human touch, our results also have implications in facilitating human-to-robot interactions. Prior efforts have worked on training robots (typically humanoid or zoomorphic) with sensor arrays to recognize different kinds of social touch expressions [11], [12], [15]. Our study complements these efforts by first uncovering quantitative data for naturalistic human-to-human touch, among people with established relationships. Via our tracking system we can obtain metrics that are not readily available from pressure sensor arrays, such as the number of fingers making contact and 3-D positioning of the hand and contact.

Aim 2: Create equipment and algorithms to extract physical quantities of touch gestures simultaneously with microneurography recordings.

Abstract—Human-to-human touch conveys rich, meaningful social and emotional sentiment. At present, however, we understand neither the physical attributes that underlie such touch, nor how the attributes evoke responses in unique types of peripheral afferents. Indeed, nearly all electrophysiological studies use well-controlled but non-ecological stimuli. Here, we develop motion tracking and algorithms to quantify physical attributes – indentation depth, shear velocity, contact area, and distance to the cutaneous sensory space (receptive field) of the afferent – underlying human-to-human touch. In particular, 2-D video of the scene is combined with 3-D stereo infrared video of the toucher's hand to measure contact interactions local to the receptive field of the receiver's afferent. The combined and algorithmically corrected measurements improve accuracy, especially of occluded and misidentified fingers. Human subjects experiments track a toucher performing four gestures – single finger tapping, multi-finger tapping, multi-finger stroking and whole hand holding – while action potentials are recorded from a first-order afferent of the receiver. A case study with one rapidly-adapting (Pacinian) and one C-tactile afferent examines temporal ties between gestures and elicited action potentials. The results indicate this method holds promise in determining the roles of unique afferent types in encoding social and emotional touch attributes in their naturalistic delivery.

Introduction

People often touch one another to convey social thought and communicate emotion. For example, one might tap the shoulder of another to get their attention, or lightly grasp and stroke their arm to congratulate them. From prior work we know that many of these gestures can be readily understood [1],

[2], suggesting the possibility that underlying neural codes, originating from the periphery, are elicited from the physical attributes delivered by another person. Various subtypes of neural afferents in the skin are thought to be involved, such as C-tactile afferents which respond to light stroking at particular velocities and at the temperature of human skin [6]. However, it is currently unknown how naturalistic human touch decomposes into low-level physical quantities that serve as direct input to neural afferents – indentation depth, shear velocity, contact area, distance to receptive field center – nor how they might be differentially parsed by the rich diversity of subtypes.

Nearly all prior efforts to characterize the response functions of human afferents to touch quantities have employed precisely-controlled mechanical stimuli, such as rigid indenters and rotating brushes [5], [6], [27], [28]. Such stimuli vary only one attribute at a time. When stroked by a brush at a range of velocities, C-tactile afferents, for example, have been found to preferentially fire between 1 and 10 cm/s, which is perceived as being pleasant [8]. By contact with a rigid probe, rapidly-adapting (RA) and Pacinian corpuscle (PC) afferents have been found to detect small amounts of contact, and encode the onset and offset of held stimuli as well as periodic vibration frequencies [28], [29]. That said, a recent effort employed natural surface textures, e.g., velvet, fleece, drapery tape, mounted to wheels rotated against the stationary fingers of primates [30]. These textures indeed attempt naturalistic interactions, yet not to the point of one person touching another.

The response properties of tactile afferents may be further elucidated by considering naturalistic and human delivered inputs in other sensory systems. In human hearing, for example, the co-modulation property of auditory neurons was found to enhance their ability to pick out tones and vocalizations amidst background animal noises [31]. In the visual system, peripheral neurons perform specific decorrelations to reduce visual redundancy that is characteristic of natural scenes [32]. These sensory systems also contain human-specific components – distinct brain regions are dedicated to recognizing human faces [33] and human voices [34] as compared to other sights and sounds. For the tactile system as well, we must consider that the response properties of peripheral nerves in the skin may be particularly tuned to the touch of another human.

When trying to measure physical contact attributes underlying human touch, devices such as sensor mats, sleeves and pads have been used [11], [12], [15]. Although using such devices can allow for high-fidelity measurement of forces and contact areas, they inhibit direct human skin-to-human skin contact. This can change both how people deliver physical gestures and how neural afferents respond. For C-tactile fibers, which respond to light shearing of the skin as well as human body temperature, such a barrier may attenuate or confound their response. The extreme sensitivity of certain afferents, e.g., slowly adapting type I (SAI) afferents that fire at forces of less than 1 mN [22], may also preclude placing any external device on the skin. For this reason, measurement techniques which do not impede skin-to-skin contact are ideal.

In order to understand how distinct populations of neural afferents in the skin might encode the complex and interdependent physical quantities that underlie natural human touch, a first step is to conduct synchronous measurement of physical contact and neural firing outputs. Towards this end, we developed a methodology to track and measure contact between a toucher's hand and the receptive field of a single peripheral afferent via a motion tracking system, while simultaneously recording trains of action potentials via in vivo microneurography [4].

Methods

Human-to-human contact, between a toucher's hand and the receiver's arm or hand, was measured using a motion tracking system consisting of both a 2-D high definition video camera and a 3-D stereo infrared device (Figure 2.1). The latter device produces highly accurate measurements of the positions of the bones of each of the joints in the hand, when it is properly recognized and stable; however, it is prone to errors in mid-identifying the hand position, especially during dynamic motion or when fingers are occluded by the hand [25]. To address these shortcomings, an additional 2-D video camera, positioned at a different viewing angle, was used along with algorithms to track the fingertips and determine proper orientations of the hand (Figure 2.1).

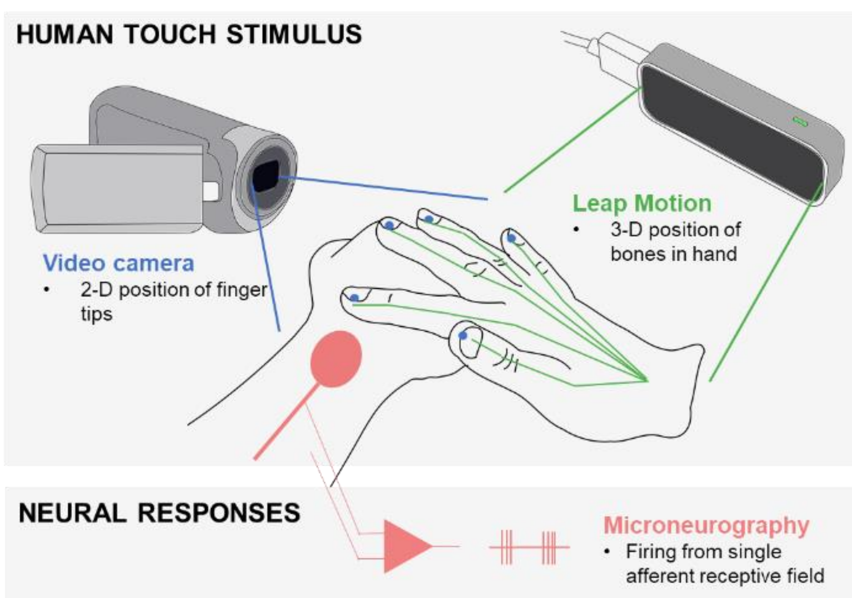

Fig 2.1) Experimental setup. The two major components for tracking human touch attributes are a video camera and a Leap Motion controller, used in tandem to track contact between the toucher's hand and the receiver's receptive field. Neural responses are measured simultaneously via microneurography.

Simultaneous to the visual observations, action potentials from single, peripheral neural afferents were recorded using microneurography. In particular, in a study with touchers and receivers, recordings were done from one C-tactile fiber and one Pacinian corpuscle fiber, in separate participants. Temporal correlations were examined afterward between the contact characteristics (as determined via motion tracking) and the neural firing.

Motion tracking components. The motion tracking consisted of two main components: a 2-D high definition video camera (HDR-CX625, 9.2 megapixel, Sony Corp., Tokyo, Japan) and a 3-D infrared stereo camera system (Leap Motion, San Francisco, CA). During experiments, while the “toucher” was contacting a participant, the positions of the bones in the toucher’s hand were measured in 3-D by the Leap Motion controller at approximately 40-60 Hz, as well as recorded in 2-D high definition video (1280 x 720 pixels) at 30 Hz. The use of both systems together afforded much better results than using either alone, as will be explained.

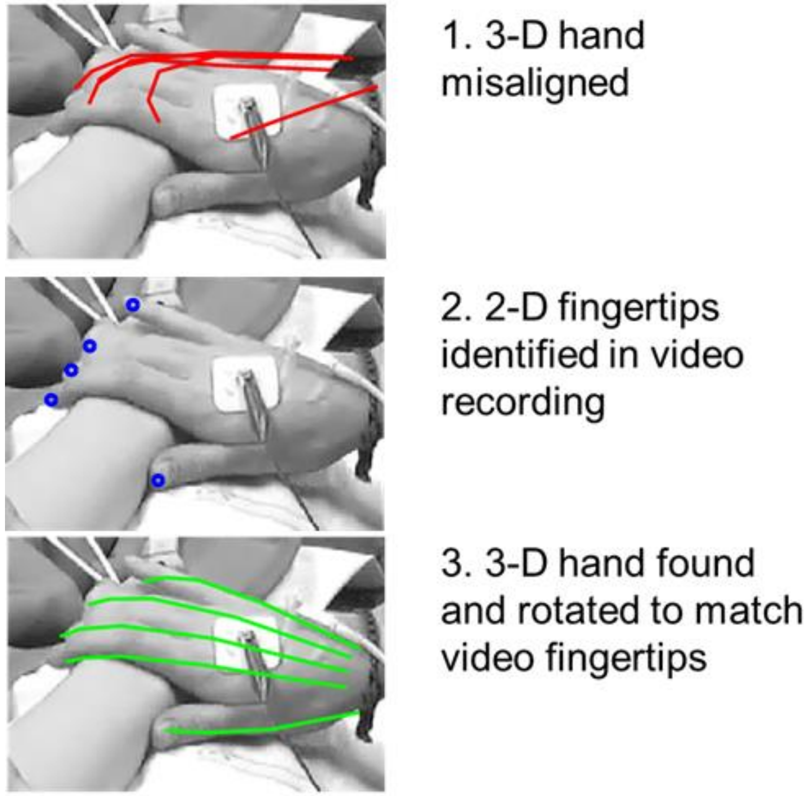

Fig 2.2) Combining 2-D video and 3-D stereo infrared data to improve overall accuracy. A series of three steps is shown beginning the 3-D stereo data which yield the positions of the bones in the hand, in this case misaligned relative to the video data. Next, the fingertips are identified in the 2-D video data. Finally, the 3-D hand in the top frame is rotated given the fingertip positions.

The first step of this process was to perform post-processing of the video data. The fingertips and palm were hand-identified in the 2-D video by a research assistant at one-second intervals. This process took approximately 5-10 minutes per minute of video. Between these hand-coded frames, a simple linear least-squares correlation filter was used to track the position of the palm and fingertips from frame to frame. Afterwards, the tracked palm and fingertips were reviewed by the research assistant along with the video data, and any notable discrepancies were fixed manually. The result was a list of 2-D locations in the video coordinates for the fingertips and palm per each frame of video (6 locations by 30 frames per second = 180 points per second of video).

The next step was to align 3-D measurements of the hand to fit the 2-D video data (Figure 2.2). Utilizing the palm locations, which were reliably measured in both the 2-D video coordinates and the 3-D Leap Motion coordinates, an affine camera matrix was fit to transform the Leap Motion coordinates to the video coordinates. In a processing program written in MATLAB, for each frame of video, fingertip locations were compared in the 2-D video coordinates (as identified in post-processing) versus the transformed Leap Motion measurements at that time. If the discrepancy between the transformed Leap Motion fingertips and video fingertips was above a certain threshold, the program would search for alternate hand configurations from prior measurements in the Leap Motion recording. For each alternate hand configuration, the program would place the alternate hand at the original palm position, and perform several 3-D rotations to it. The best hand configuration was chosen as the pair (hand configuration, rotation) that best fit the 2-D video fingertip data. The result of this process was a set of "toucher" hand measurements in 3-D space that matched the video much more closely than the original Leap Motion recording.

Fitting the local region of the receptive field. After the 3-D finger and hand measurements had been properly matched to the 2-D video recordings, the location of the receptive field was identified in 3-D. Based on the hand marking on the receiver's arm that corresponded to the receptive field center, frames of video in which the index finger crossed over the receptive field were selected. A plane was fit to the 3-D positions of the index finger for these frames, with the center at the mean coordinates. A local region of skin surrounding the receptive field was modeled as a circular region of this plane with a radius of 3 cm. In subsequent measurements, contact was only considered if it lied within this local region.

Measuring contact with the receptive field. Hand position data from the Leap Motion resulted in 3-D poses, widths, and lengths for each bone in the hand (Figure 2.3). In custom software, written in Python 2.7, these were translated into cylinders made up of 3-D line segments. Each intersection between these lines segments and the plane representing the receptive field was treated as a contact point.

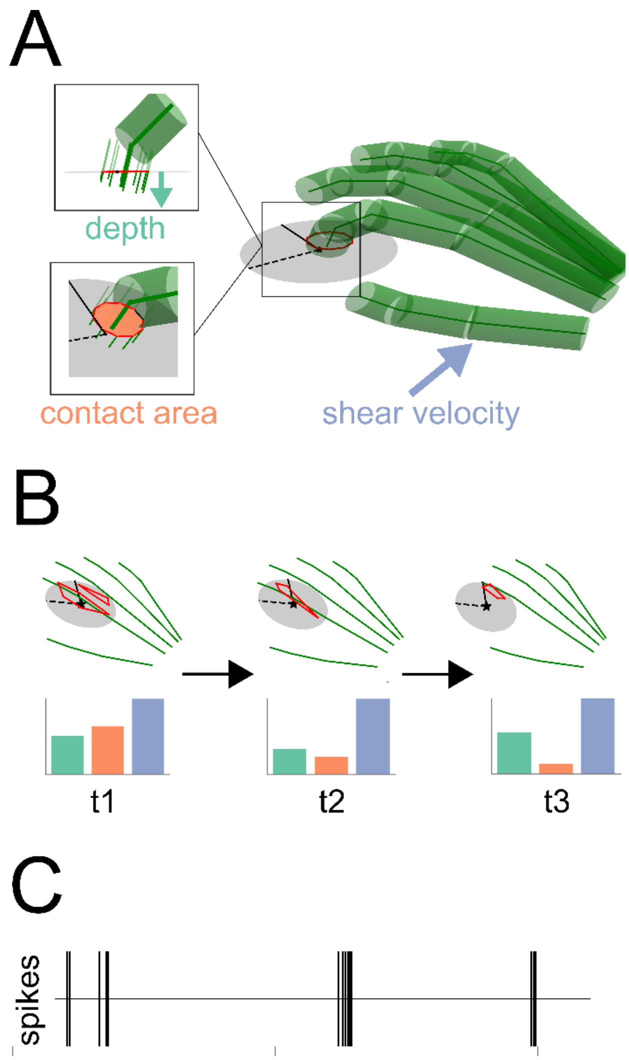

Fig 2.3) Measuring contact near the afferent's receptive field along with elicited neural spikes. A) Three physical quantities are shown as measured by the tracking system: mean indentation depth, contact area, and shear velocity. Note that the fingers are represented as cylinders, formed by multiple line segments, as shown in the "depth" panel. Their intersection with the plane forms contact points which are connected to estimate contact area. B) Three distinct time points are shown for contact made by a stroking gesture, with relative levels of each physical quantities, associated by hue from panel A). C) Neural spike times as measured via microneurography for a multi-finger stroking gesture.

We examined four quantified touch attributes, which had been considered in prior work [35], [36]. The attributes of 1) contact was determined as a binary value representing whether any bones from the toucher's hand intersected with the receptive field plane. 2) Depth was measured as the mean of the normal distance from the plane to the end of each contacting line segment per bone of the hand. 3)

Contact area was measured as the area of the convex hull enveloping the contact points for each bone in the hands. 4) Shear velocity was measured as the mean velocity of each contacting fingertip (or palm) tangent to the local receptive field plane.

Human-subjects experiments. *Participants.* Two participants took part in this study (ages 34 and 27, both female). Informed consent, in writing, was obtained before the start of the experiment. The study was approved by the ethics committee of Linköping University (Dnr 2017/485-31) and complied with the revised Declaration of Helsinki.

Experimental design. In each experiment, a trial-set of four gestures were performed to the receptive field of a single-unit neural afferent. 1) Single-finger tapping: the toucher delivered three sets of 3-6 taps, directly on top of the receptive field. 2) Multi-finger tapping: the toucher tapped continuously with 3-4 fingers, while moving the entire hand back and forth across the receptive field. 3) Multi-finger stroking: the toucher performed 3 broad strokes in succession across the receptive field of the afferent using 3-4 fingers lying flat against the skin. 4) Whole-hand holding: the toucher laid the hand down flat onto the receptive field, mostly contacting with the fingers with slight contact of the palm, and a very light squeezing. These standardized gestures were applied by trained experimenters. The experimenter received spoken cues via headphones, first the cue-word, then a countdown (3, 2, 1, go). They were instructed to perform the touch starting from the "go" signal until they heard a stop signal (3, 2, 1, stop), creating a continuous time window of touch for 10 seconds. The toucher was familiarized with the neuron's receptive field and required to touch an area of skin including but not limited to the receptive field. Gesture data for 2 trial-sets for the C-tactile fiber and 1 trial-set for the Pacinian corpuscle were obtained. Each gesture lasted a total of 10 seconds. The exact execution of each gesture was kept somewhat vague, in an attempt to deliver a more natural and volitional stimulus.

Microneurography. Microneurography is a long-standing, safe, and painless procedure for recording from single peripheral afferents in awake, unanesthetized participants [37]. The participants were seated in a comfortable chair and pillows were provided to ensure minimal discomfort. All recordings were made from the right radial nerve. As a first step, the radial neve was visualized using the ultrasound technique (LOGIQ e, GE Healthcare, Chicago, IL, USA). Then, a recording electrode (FHC, Inc. Bowdoin, ME, USA) was inserted percutaneously followed by localization of the nerve by electrical stimulation through the recording electrode. Minute movements were made to the recording electrode, manually or with a pair of forceps, until single-unit activity could be recorded. In addition to the recording electrode, an indifferent (uninsulated) electrode was inserted subdermally, approximately 5 cm away from the nerve.

After the recording electrode reached a stable position for single-unit recording, each neuron was classified by its physiological characteristics, as per the criteria used in [38]. Neural recordings were performed with equipment purpose-built for human microneurography studies from AD Instruments (Oxford, UK) or the Department of Integrative Medical Biology, Umeå University (Sweden).

All neural data were recorded and processed using LabChart Pro (v8.1.5 and PowerLab 16/35 hardware PL3516/P; AD Instruments, Oxford, UK) or SC/ZOOM (Department of Integrative Medical Biology, Umeå University). Action potentials were distinguished from background noise with a signal-to-noise ratio of at least 2:1, and were confirmed to have originated from the recorded afferent by a semi-automatic inspection of their morphology [22].

Results

Example physical attributes identified from one set of each of the four gestures are shown in Figure 2.4. For one finger tapping, there were relatively small amounts of contact area and shear velocity, with changes in depth in concert with each tap. For multi-finger tapping, contact area was slightly greater with multiple fingers contacting at once, with a greater frequency of taps compared to the one-finger tapping.

In the multi-finger stroking gesture, depth remained consistent, as both shear velocity and area increased the fingers swept across the receptive field. Finally, in the whole-hand holding gesture, depth and area remained constant, with minimal shear velocity.

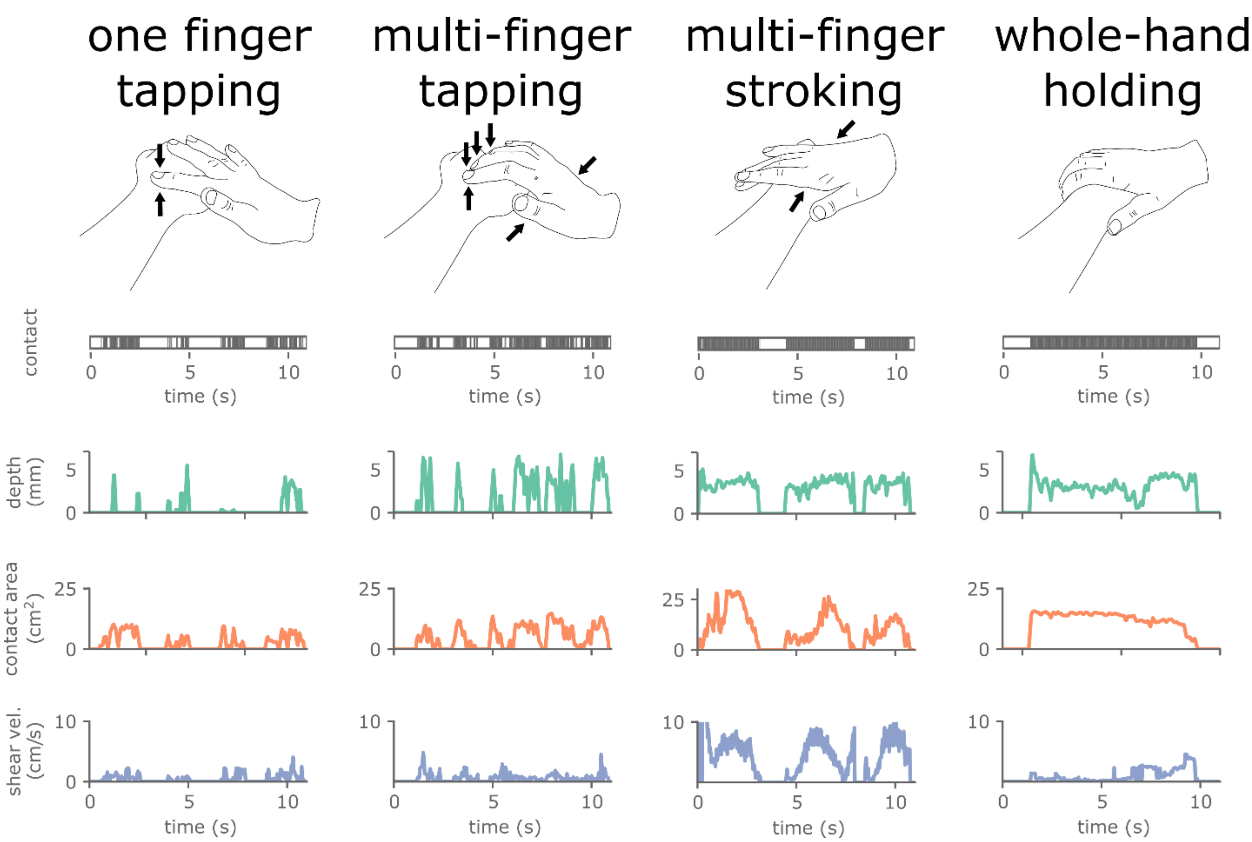

Fig 2.4) Example physical contact data for each of the four gestures. Physical contact measurements are shown for each of the four gestures over 10-second time windows. Short bursts of depth along with low contact area and shear velocities are characteristic of the one-finger tapping gesture. The multi-finger tapping gesture resembles the one-finger tapping except with greater contact and contact area and a small shear velocity component as the toucher moved across the arm. The multi-finger stroking gesture generally contained three strokes of about 3 seconds each, with consistent depth as well as high amounts of contact area and shear velocity. The whole hand holding gesture consisted of long, continuous contact with large contact area and low shear velocity.

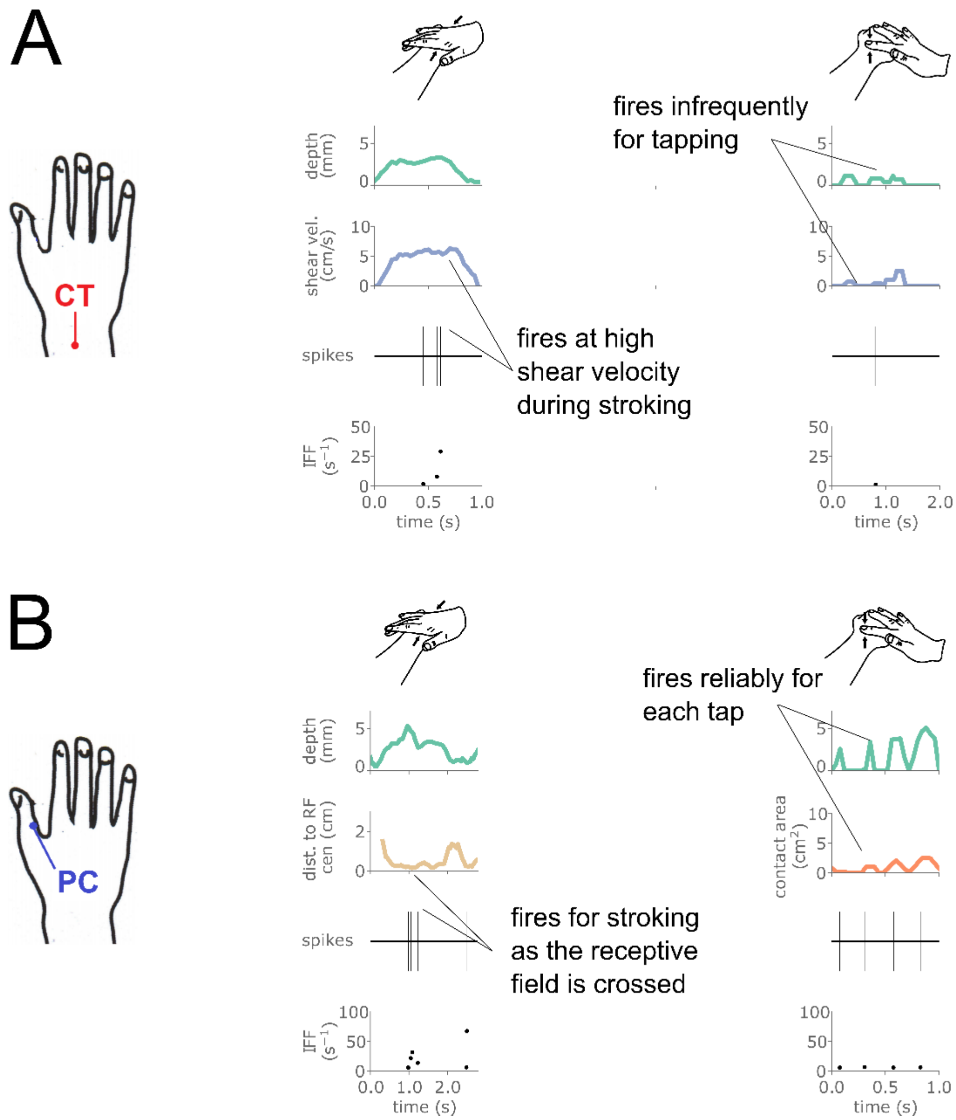

Fig 2.5) Responses of neural afferents to the physical quantities of human touch. A) Depicts the firing of the C-tactile afferent under a few example conditions during the experiments. During a stroking gesture, the afferent responded to the high shear velocity (left); when being tapped, the afferent fired infrequently (right). B) Depicts the firing of the PC fiber to similar example conditions during the gestures. During a stroking gesture, the PC afferent fired in short bursts as the receptive field was crossed (left); during tapping, the PC fired synchronously with each tap (right). For both afferents, the position of the receptive field on the touch receiver's arm/hand is illustrated.

Example neural responses for the C-tactile afferent are shown in Figure 2.5A. The C-tactile afferent fires mostly during the long stroking from the multi-finger stroke gesture, when both shear velocity and contact area are large. The ranges of velocities employed by the toucher matched the peak response range of C-tactile afferents from brushing experiments, 1-10 cm/s [8]. During tapping, the C-tactile afferent fired rarely if at all. Peak firing rates for the C-tactile afferent over all gestures were during the multi-finger stroking, at a maximum frequency of 44 Hz (Figure 2.6).

Example neural responses for the PC afferent are shown in Figure 2.5B. For one-finger and multi-finger tapping, the PC afferent fires synchronously with each tap. For stroking, however, the PC afferent fires only as the stimulus crosses the center of its receptive field. Peak firing rates for the PC afferent over all gestures were during multi-finger tapping, at a maximum frequency of 362 Hz (Figure 2.6).

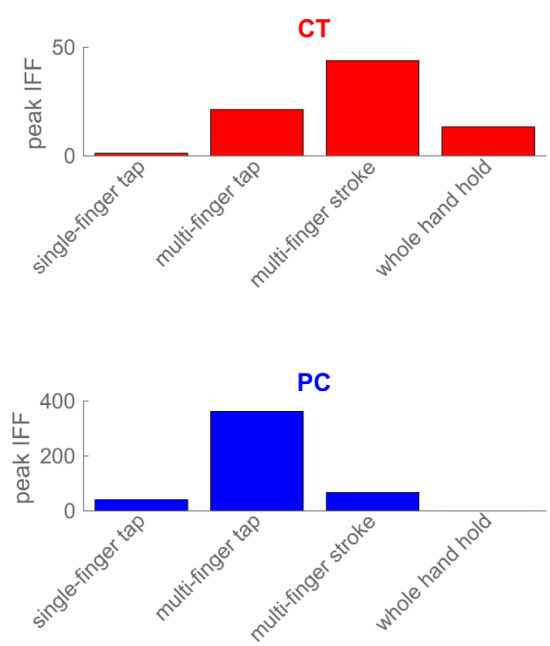

Fig 2.6) Peak firing rates per gesture. The C-tactile afferent (Top) fired at the greatest frequency (43.8 Hz) during the multi-finger stroke, while the PC afferent (Bottom) fired at the greatest frequency (362.3 Hz) during the multi-finger tapping.

Discussion

To our knowledge, this effort is the first to report methods that allow natural human-to-human gestures to be delivered and tracked as stimulus input simultaneous with single afferent microneurography. Nearly all prior microneurography studies have employed a classical stimulus-response paradigm [5], [6], [8], [28], [29], [38]. The use of non-contact stimulus tracking is a paradigm shift where we allow natural movements and contact interactions as desired by the human toucher, and seek only to track what occurs, for post experiment correlation with the neural response. Our preliminary examination of C-tactile and PC responses align well with prior literature and suggest that each afferent type may encode unique aspects of human touch.

To quantify human touch during the neural recordings, we decided to use an optical, camera-based motion tracking system. Sensor mats, sleeves, and other physical components create barriers between skin-to-skin contact and thereby alter the delivery of gestures as well as the neural responses. We found a combination of the Leap Motion IR camera system along with 2-D video recordings to offer the best accuracy given the constraints of other devices and those of the microneurography environment. In the future, using pressure-sensitive devices in separate experiments may allow us to better inform the "depth" metric in our contact modeling to represent real pressure distributions from human touch.

In our preliminary neural recording data, we observe trends in the response properties for both the C-tactile and PC afferents that align well with the literature. In terms of encoding human touch, we observe that the C-tactile afferent responds most to light stroking, while the PC afferent responds synchronously with tapping gestures, as well as the onset of contact with the receptive field during stroking. Of course, with a sample size of two, these findings are preliminary and require further studies with a greater number of afferents and subtypes.

Unlike traditional methods of controlling stimuli, in which a single factor is varied at a time, the naturalistic touch inputs simultaneously include several factors. Some of the covariance between these factors may be inherent to human touch and help elucidate neural encoding patterns—as neurons in the visual system decorrelate redundancy that is characteristic of natural scenes. Likewise, it is possible that tactile neurons are tuned to inherent dependencies in the physical primitives that underlie human touch. In particular, metrics such as contact area and indentation depth may be intimately related—a finger pressing more deeply into the arm will contact with a greater area. Multivariate statistical analyses or machine learning techniques may prove useful in examining these types of complicated, multi-factor relationships. Constructing such relationships is key to further understanding our innate ability to decipher the touches from another human.

Acknowledgment

We would like to thank Dr. Ewa Jarocka at the Department of Integrative Medical Biology (IMB) at Umeå University for her assistance in performing the microneurography experiments.

Aim 3: Determine how systems of Aβ and C-tactile afferents encode touch expressions and their underlying component gestures.

Abstract—Social and emotional sentiment is often conveyed through physical expressions of touch. Although we are now beginning to understand and quantify the physical contact underlying these expressions—e.g., force, velocity, contact duration—it is unclear how these touches are encoded by first-order neurons, or exactly how they might integrate to form an emotional percept. In a novel experimental paradigm, we applied naturalistic human touch stimuli, a set of 6 touch "expressions," in combination microneurography and motion tracking experiments with 7 afferent subtypes (44 units in total). Simple features of the neural response to these expressions—such as peak firing rate, mean firing rate, and number of spikes— were found to be statistically differentiable within a single hair follicle afferent (HFA) or slowly-adapting type II afferent (SA-II). The high acuity these afferents afforded in discriminating human touch appears to stem from their unique and robust responses to the component gestures underlying each expression. In the C-tactile (CT) system, we found firing frequencies to well align with the perceived pleasantness of each touch expression, suggesting a complementary role in modulating the affect of each expression. The perceptual significance of these first-order responses requires further study, but the results raise the possibility that tactile social and emotional information may be encoded very distally in the periphery.

Introduction

Touch is an often-used medium for conveying social thought or communicating emotions. For example, one might lightly tap another to get their attention, or stroke their arm to calm them. Some of these expressions can be inherently understood [1], [2], [36], [40], suggesting that there may be neural circuitry in place to decode emotional and social touches. As we seem to be particularly tuned in other sensory systems to human inputs, such as our ability to uniquely recognize human faces [33] and voices [34], there may be the possibility that certain neural responses are tuned towards recognizing human touches. However the role of each specific unit, or how they might integrate together to form an emotional percept, is yet unknown.

Through qualitative, observational studies, it has been shown that touch is effective at communicating several emotions including anger, happiness, and sadness [1], [2], [41]. In recent studies, we have utilized motion tracking systems and basic contact models to more quantitatively assess how people naturally perform touch expressions at the level of skin contact. We have found some touch expressions to be understood more intuitively than others [36], including some like “attention” which are innately understood to a very high degree. Understanding how the physical contact underlying these expressions can elicit neural responses may further elucidate why they are immediately recognizable.

The discriminative touch domain of the Aβ classes of afferents has been well characterized. Distinct afferent types encode perceptions of pressure, vibration/texture, stretch, and the displacement of hair follicles. Indeed, sensations of such elementary components of pressure and flutter/vibration can be caused via electrostimulation of a single nerve ending [42], [43]. However, it is unclear how more complex touch gestures, involving multiple elementary sensations, are signaled from the periphery.

Another class, the C-tactile afferents, are thought to play a significant role in social touch perception [44]. These afferents respond to low mechanical forces of 0.3-2.5 mN, have slow conduction velocities of 0.6-1.3 m/s [27] and project to insular cortex [6]. They appear to be tuned to specific velocities encountered in light, stroking touch [6], [45], and correlate with the perceived pleasantness of touch. They also fire preferentially for applied temperatures similar to those of human skin [7]. However, as of yet their responses have not been characterized to the application of real human touches.

In the current study, using in vivo electrophysiological technique of microneurography [4], we recorded the responses of single afferents, belonging to each of the somatosensory channels, to naturalistic, complex touch gestures that resemble those used in real inter-personal communication. During stimulation, the physical attributes of social-touch gestures were measured and characterized using video recordings and a real-time motion tracking system. Statistical and machine learning analyses were further used to characterize the capability of each afferent type to differentiate the set of touch expressions.

Results

In order to understand how emotional and social expressions of touch might be differentiated at the single-unit level, we performed microneurography experiments with naturalistic touch inputs, and further quantified touch contact with a motion tracking system [26]. Our results indicate that single Aβ fibers, namely hair-follicle afferents (HFA) and slowly-adapting type II afferents (SA-II) were able to well differentiate the gestures, via statistically significant differences in aggregate metrics of their firing rates. We also noted robust and unique responses of these types to component gestures underlying each expression. Finally, the C-tactile system was found to correlate positively with the perceived pleasantness of the touches.

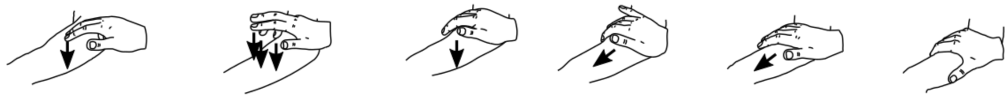

	attention	happiness	gratitude	calming	love	sadness
tapping	short	long				
patting			short			
stroking				short	long	
holding			short			long

Figure 3.1) The 6 touch expressions and their physical gestures classified into components of "tapping," "patting," "stroking," or "holding." More detailed temporal information can be seen in Figure 3.4.

First, by both visual inspection and quantification with a custom motion tracking system (see Methods), we decomposed our standardized touch expressions into 4 physical gestures (Figure 3.1). "Attention" was comprised of tapping, in 4 short bursts of 4-5 taps. "Happiness" was also comprised of tapping, but was more continuous, using multiple fingers and moving up and down the arm. "Gratitude" consisted of alternating patting and slow holding on the arm. "Calming" and "love" were both stroking gestures, with calming consisting of 4 short strokes down the arm and love consisting of continuous back-and-forth stroking down the arm. "Sadness" was a sustained hold on the arm with some light squeezing. More detailed temporal information can be seen in Figure 3.5.

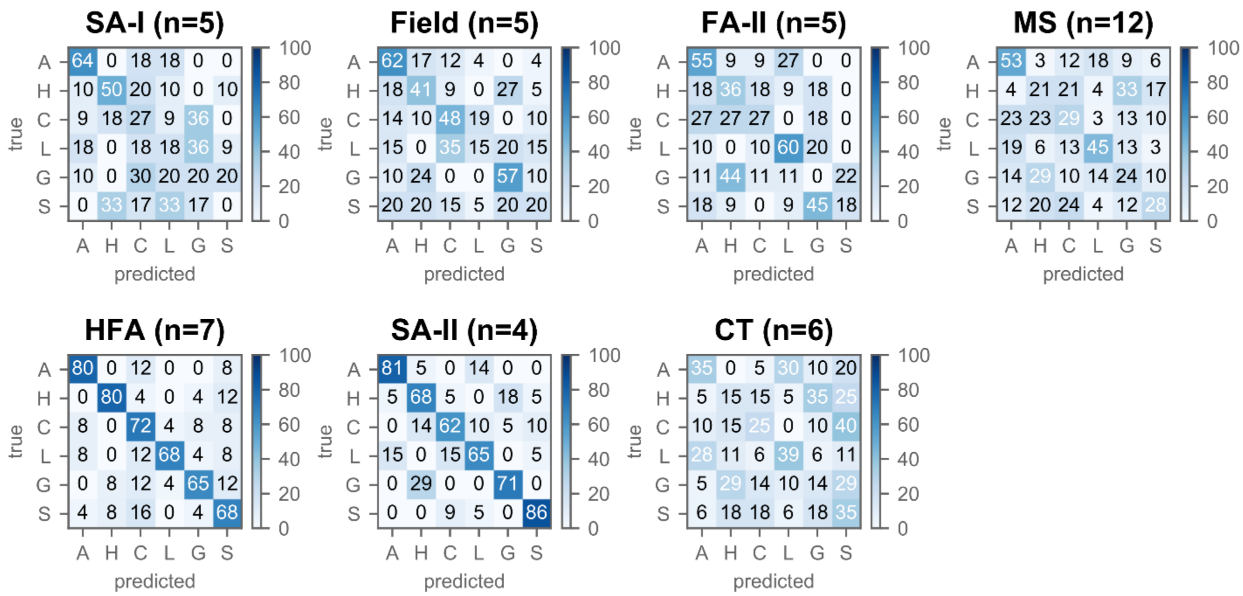

Figure 3.2) Differentiability of touch expressions via single-unit responses. A random forest classifier was fit to 5 features of neural firing for each afferent type. Next, a 5-fold cross validation procedure was used to determine the confusion matrices (values are a percentage of the true word classified into each column). The 5 features of the neural signal used in the model were: 1) max firing rate, 2) mean firing rate (when a spike occurred), 3) standard deviation of firing rate, 4) total number of spikes, and 5) number of bursts (number of inter-spike intervals > 1 second). Classifiers using the HFA and SA-II firing features exhibit notably strong accuracy as compared to the others. Chance accuracy was 16.7%. A: attention, H: happiness, C: calming, L: love, G: gratitude, S: sadness.

Using a random forest classifier, we examined which afferents types were capable of differentiating the social touch expressions via 5 features of their firing rate (Figure 3.2). The hair-follicle afferents (HFA) and slowly-adapting type II afferents (SA-II) were the strongest differentiators, each with 72% overall classification accuracy. Of the other afferent types, most were able to classify some subset of the touch expressions well, such as “attention,” and “happiness” by the slowly-adapting type I (SA-I) afferents, and “love” by the fast-adapting type II (FA-II) afferents. The C-tactile (CT) afferents exhibited the lowest classification accuracy at the single-unit level, with an overall accuracy of 26%. Notably, all of the afferent types were reasonably accurate in classifying the “attention” expression.

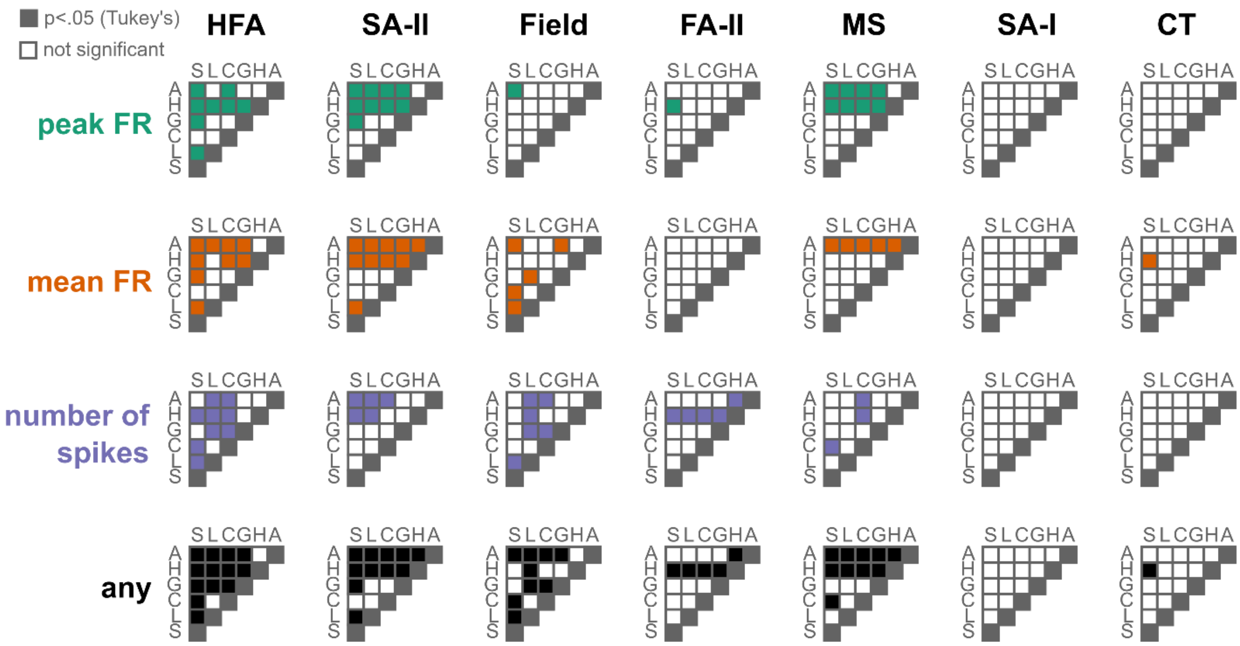

Figure 3.3) Neural firing features which distinguish the expressions for each afferent type. The top three rows each examine a different metric related to the neural firing: peak firing rate, mean firing rate, and the number of spikes. Filled-in squares denote that a significant pairwise significant difference was determined, via ANOVA and Tukey's HSD post-hoc ($p < .05$). If a significant difference was found across any of the metrics in the first 3 rows, that pair is designated with a filled-in square in the final row "any." A: attention, H: happiness, C: calming, L: love, G: gratitude, S: sadness.

After the machine learning analysis, we performed a statistical analysis to examine which features of the firing rate were differentiable (Figure 3.3). Peak firing rate, mean firing rate, and the total number of spikes each afforded similar levels of differentiability, although mean firing rate had the most significant differences across all the afferents. The differences in these 3 features seem to account for much of the prior classifier's accuracy. Again, the HFA and SA-II were able to distinguish the most gestures (all but 2 pairs for the HFA, and all but 4 pairs for the SA-II).

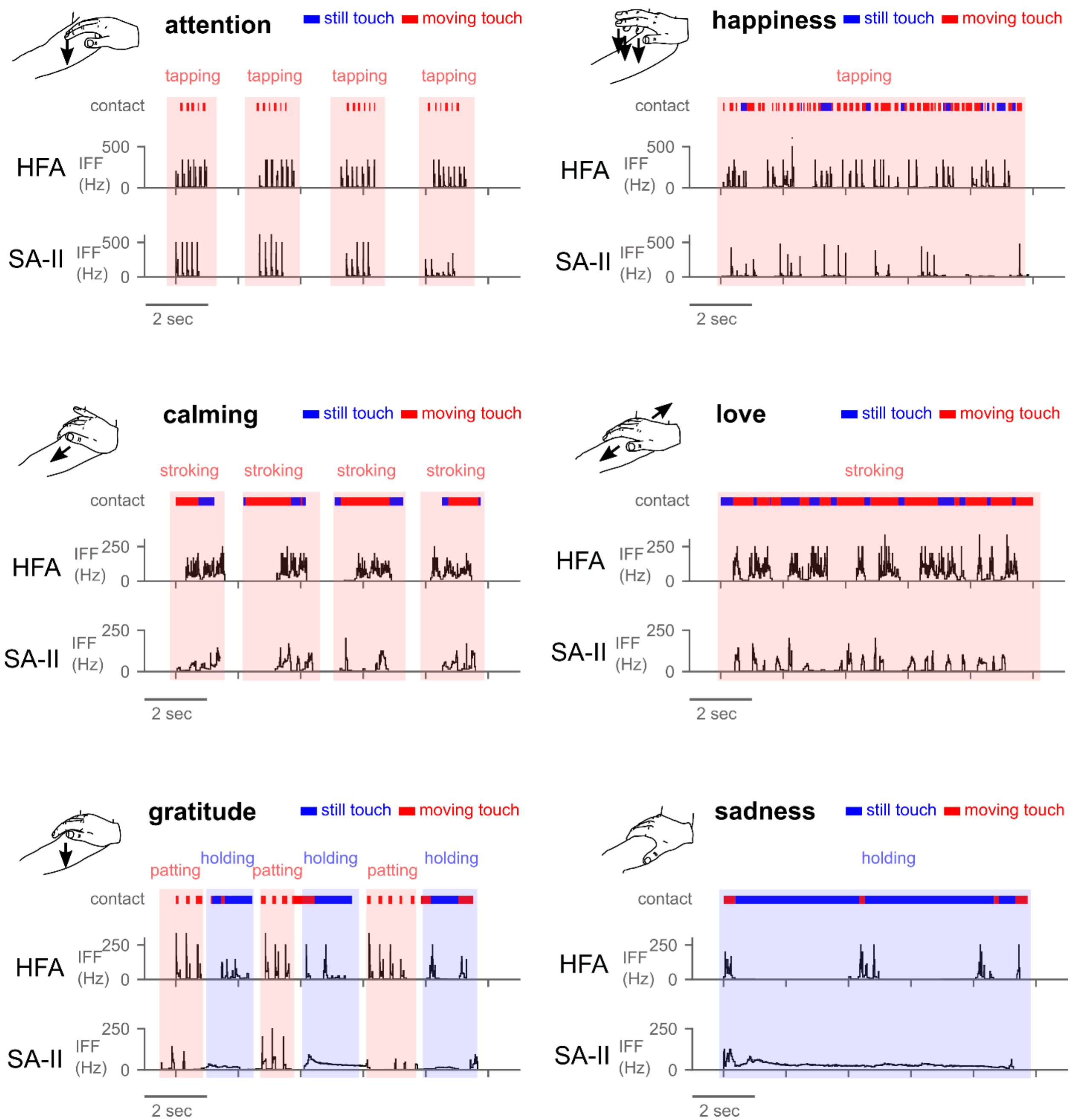

Figure 3.4) Temporal encoding of the touch expressions by HFA and SA-II afferents. Each row compares two touch expressions with similar physical component gestures. Within each panel, contact is being made is designated at the top as either "still" or "moving," as quantified by our custom tracking system. The contact is further binned into the 4 component gestures of tapping, patting, stroking, and holding. Instantaneous firing rates for exemplar HFA (top) and (SA-II) afferents are shown below the contact. The neural recordings and physical contact in this figure are asynchronous, but are aligned so as to be representative of the physical input to the neurons at any given time.

In Figure 3.4) we examined the neural firing rates of the HFA and SA-II responses along with exemplar contact data from a custom motion tracking system. For “attention,” both the HFA and SA-II afferents responded with short, high-frequency bursts of firing well matched to each tap. Similar responses were seen in the tapping during “happiness,” although the SA-II was not able to capture as many of the taps. For “calming” and “love,” both afferents responded with sustained, medium-rate firing during each stroke, but with a longer duration for “love.” The patting sections of “gratitude” caused responses in both afferents similar to tapping but with lower firing frequency. Holding was the only gesture encoded differently by each type—the HFA did not respond during the hold, only on the onset or offset (or when the hand was readjusted), while the SA-II responded with low-rate, sustained firing. The firing patterns during each of these 4 gestures (tapping, patting, stroking, and holding) appear to be robust to the large amount of variability of the component gestures (Figure 3.5), which was not the case for the other afferent types, which varied significantly between units. The response properties of the HFA and SA-II were also more consistently differentiable than those of the other afferent types (Figure 3.6). Using another random forest classifier, but for each gesture as opposed to each touch expression, we saw an overall classification accuracy of 64% for the HFA and 61% for the SA-II afferents (chance accuracy was 25%).

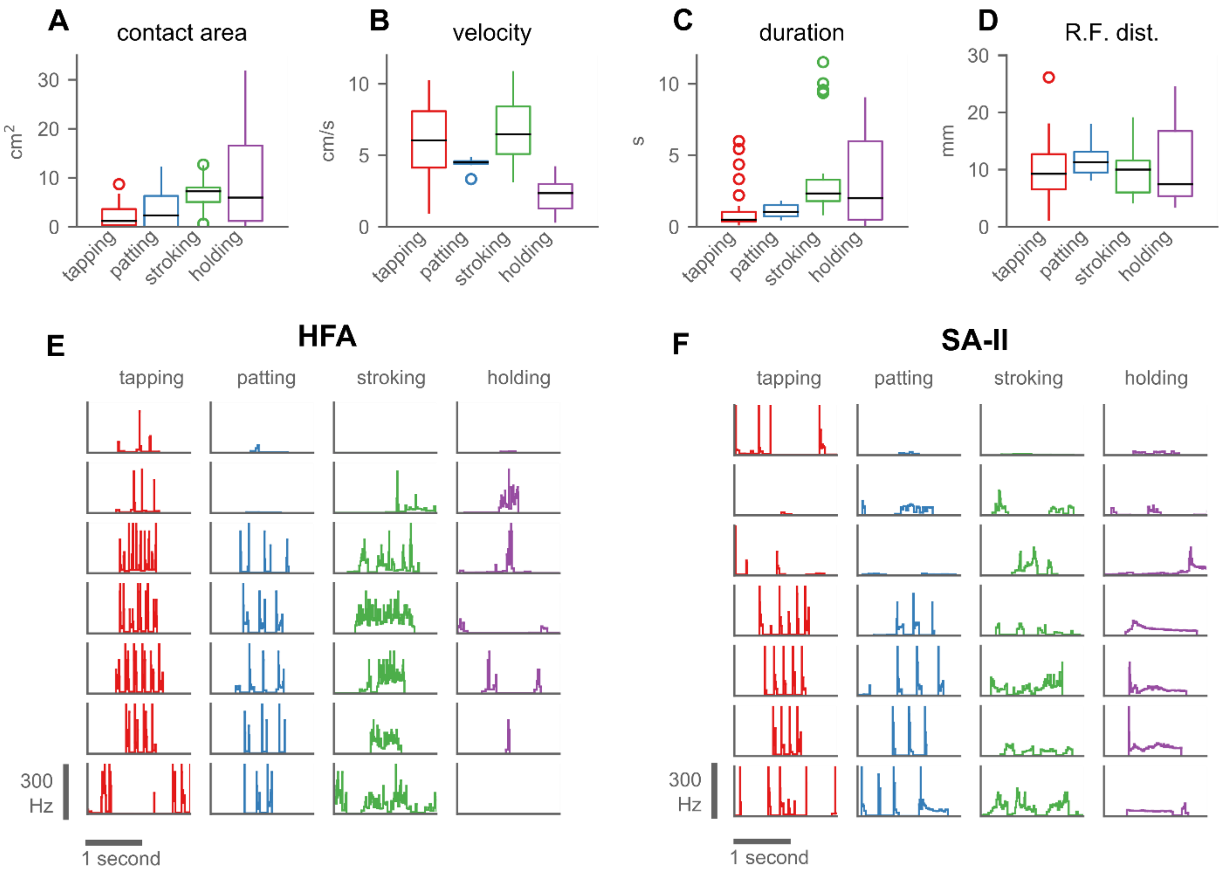

Figure 3.5) HFA and SA-II afferents have consistent firing patterns for the component gestures, amidst significant variability in the physical contact primitives. A-D show distributions of 4 contact parameters for each of the component gestures, showing a large variability in how they were performed. E and F show several randomly-chosen firing patterns for each component gesture for the HFA and SA-II afferents, respectively. These firing patters were selected across all of the measured afferents and came from separate trials, and thus are representative of the responses of all the afferents of that type. Although some of the firing patterns were longer than 2 seconds (some as long as 10 seconds for a hold, for example) only 2 seconds are shown.

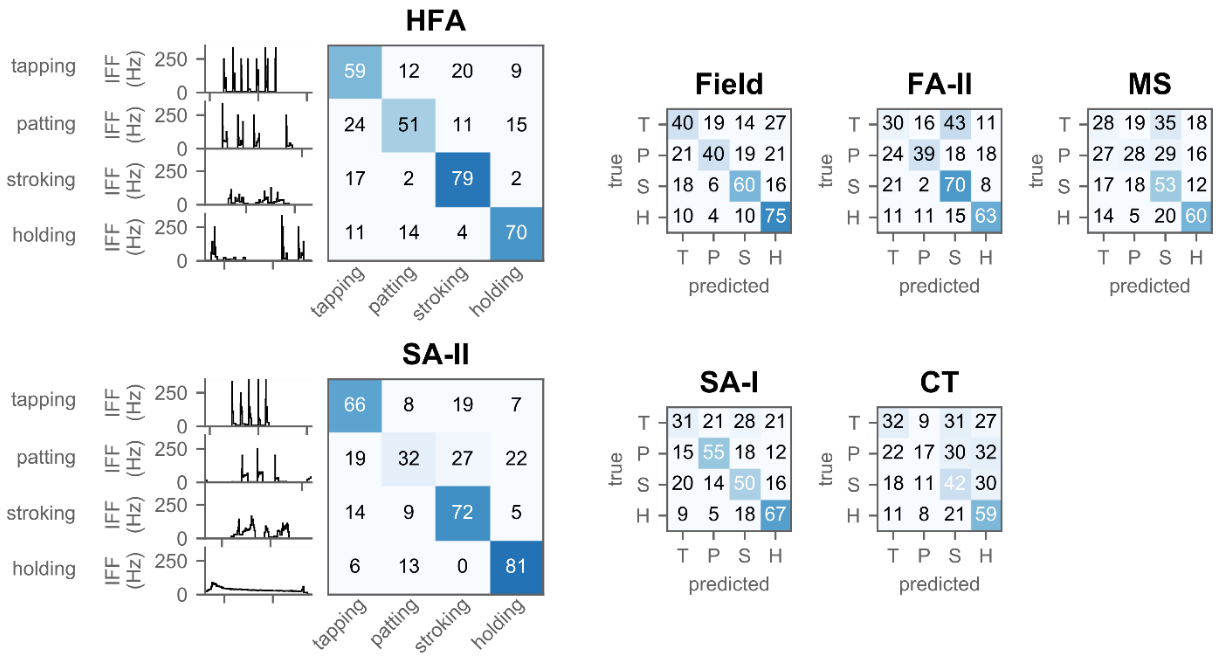

Figure 3.6) Firing patterns of the HFA and SA-II are able to differentiate each component gesture.
In each panel, to the left is shown a typical IFF time course that encodes each of the gestures. To the right, a machine learning (random forest) classifier was trained on each of these physical gestures, based on the relative times of spikes in the recordings as compared to the exemplar gestures in Figure 3.4. Confusion matrices are determined via a 10-fold cross-validation procedure, and display the classification percentages per row. T: tapping, P: patting, S: stroking, H: holding.

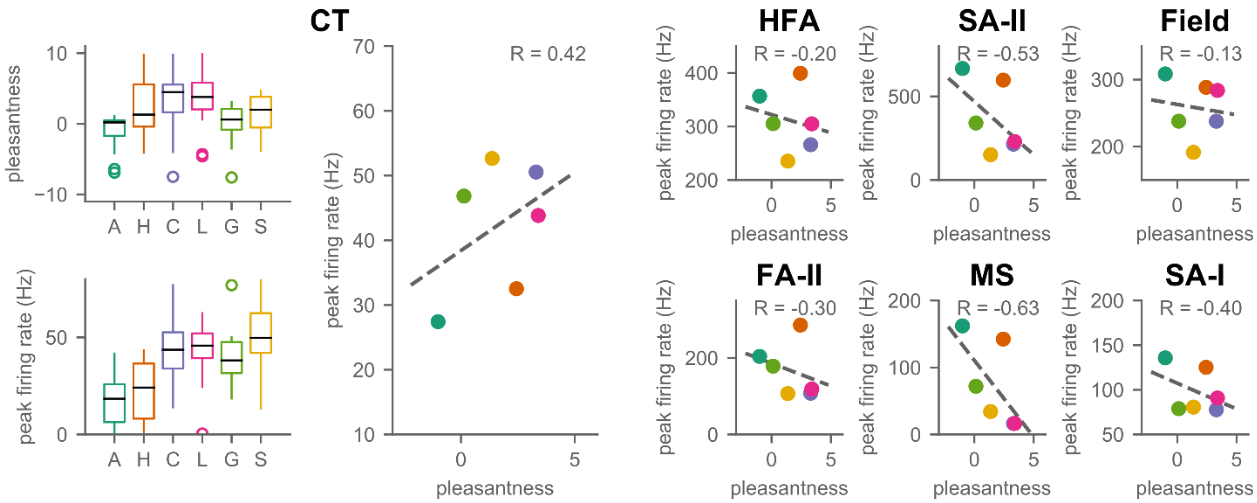

Figure 3.7) Peak firing rate of C-tactile afferents relates to the perceived pleasantness of each touch expression. A) shows the pleasantness ratings from the second, psychophysical experiment. B) depicts the distribution of peak firing rates for each touch expression for recordings from the C-tactile afferent. C) Shows the correlation between the grand mean of peak firing vs. the mean of perceived pleasantness for each touch expression. D) shows this same relationship but for the other afferent types. Notably, none of the Pearson R correlations were found to be statistically significant ($p < .05$). A: attention, H: happiness, C: calming, L: love, G: gratitude, S: sadness.

In a separate experiment, we recorded pleasantness ratings from each touch expression (Figure 3.7). All of the touches except for "attention" were rated at least mildly pleasant, with "love" rated as the most pleasant. We found a positive linear relationship between pleasantness and peak firing rate for the CT afferents (R = .42), but not for any of the other subtypes, which had negative correlations.

Discussion

This work is, in the authors' knowledge, the first to examine human-to-human touch as a stimulus in microneurography experiments. We found strong evidence that social touch expressions can be differentiated by a single-unit Aβ afferent in the periphery, namely for hair follicle afferents (HFA) and slowly-adapting type II afferents (SA-II). Other Aβ afferents likely play a significant role at a population level, such as slowly-adapting type I afferents (SA-I) which provide much of our fine touch sensation [29],

[46]. Among other afferent classes, we found continued support for C-tactile mediated affect in touch [8], noting a positive correlation between the perceived pleasantness of each perceived gesture and the peak firing rate. The muscle spindle afferents also may play a role in perception: they fired at high rates for the tapping expressions of "attention" and "happiness" as compared to the other expressions. Overall, it seems that Aβ and C-tactile afferents have complementary roles in discriminating touch expressions and modulating their affect, respectively. These data further suggest the possibility that human affective and social touch may be encoded very distally in the periphery, as differentiation of touch gestures is theoretically possible from single first-order responses.

Touch expressions can be differentiated by single units. Two afferent types stood out in their ability to differentiate our six touch expressions, the HFA and SA-II. One probable feature is the receptive area: both afferents have large receptive fields as compared to some of the other Aβ afferents, such as the SA-I and FA-II, which meant that they would more consistently respond to features of each touch gestures [29], [38], [47]. Furthermore, as these types respond to hair movement and skin stretch, respectively, the range at which they might respond is even greater. Another important factor is likely the force sensitivity functions of these subtypes. For example, the Field afferents, which had similar responses to the HFAs, were less effective differentiators as their firing frequencies were not modulated between the component gestures—the response was more "on" or "off." The modulation of peak frequency of the HFA and SA-II also allowed them to differentiate between moving touch and still touch: the HFA responded only to moving touch and not to still touch, and the SA-II responded at significantly lower frequencies for still touch. Lastly, both the HFA and SA-II were able to follow high-frequency tapping at high rates, which was not characteristic of all of the afferent types. Although these two afferent types seemed particularly good at the single-unit level, further study is required to contextualize the other afferents at the population level.

One surprising finding was that the SA-I did not appear to be as good a differentiator as an SA-II, at the single unit level. One difference may be the skin stretch response of the SA-II giving it a large receptive range. As the SA-I only responded as the receptive field was crossed during a stroking gesture, this may have made it more difficult to distinguish from a tap of similar force. It is also possible that the SA-I is too sensitive to perform this task alone. Many of the gestures varied significantly in their force, distance to the receptive field, and velocity—although the SA-II and HFA had differentiable patterns across this variability, the SA-I seems to have responded matching this variability. We did note that, at the gesture level, the SA-I was a rather effective differentiator. Further study is required to analyze the role of the SA-I at the population level.

C-tactile afferents. We had initially expected the C-tactile afferent to be a strong differentiator of human social touches, given its specificity towards light stroking of a particular frequency [8]. However, we found the C-tactile afferent to respond to all of our touch expressions at relatively high frequencies. In a secondary experiment, we found that almost all of the gestures were rated as “pleasant” by human participants, which may be why the C-tactile response was not particularly discriminative. Our understanding of the C-tactile system may be lacking some subtleties of light touch interactions, such as responses to more punctate stimuli like tapping.

Social and emotional touch encoding. It is not yet understood how emotional percepts might be formed from touch gestures, although we found evidence that this process may happen more distally than expected. When placing our emotional touches on axes of dominance, valence, and arousal [48], [49], we note that “happiness” and “attention” are particularly high arousal. Both were differentiable from the other expressions by almost every afferent type, which generally responded at high frequencies to the tapping gestures in these expressions. Therefore, we might assume that many of the afferents respond with high frequency in relation to “high arousal” gestures. The C-tactile afferents likely play a role in encoding the valence of each touch—however, it was found that low-valence expressions such as “sadness” were still perceived as pleasant in the form of touch. Further exploration of the emotional context of touches needs to be pursued to fully capture the content of these expressions.

Stimulus-response paradigm for microneurography. Unlike traditional methods of controlling mechanical stimuli, we employed naturalistic touches as our stimuli. We believe this methodology is critical in further exploring the response properties of afferents in a natural context. For instance, SA-II and CT have been thought to encode skin stretch and stroking, respectively, but we found them to respond quite well to tapping gestures. Without well-controlled stimuli, we resorted to motion tracking and modeling to quantify mechanical inputs for later analysis. We ended up using optical systems for this tracking, in order to both preserve direct skin-to-skin contact and minimally interfere with the microneurography recordings. However, as opposed to sensor pads or other sensors, these systems were not perfectly accurate, and could not measure direct quantities such as the forces of each gesture. We also had difficulties with data analysis—traditionally controlled stimuli typical vary a single factor at once, such as stroking velocity, temperature, or force; however, our naturalistic inputs co-varied many factors at a time. In addition, many of these co-dependencies, which might be perceptually relevant, were inherent to natural gestures—for instance, all of our “tapping” gestures had both high velocity and also small contact areas. We embraced these co-variances by instead looking at the component gestures as a whole, instead of reducing them to their physical primitives. Multivariate statistical analyses and machine learning techniques also proved useful in examining these types of complicated, multi-factor relationships, and suggest that there is future promise in characterizing neural responses to naturalistic stimuli.

Methods

Participants—touch receivers. All participants were recruited through local advertisement and a mailing list. Using the microneurography technique for single-afferent axonal recordings (11), responses to social-touch gestures were recorded from 44 low-threshold primary afferent fibres belonging to the right radial nerve in 12 healthy participants (23-35 years; 7 males, 5 females). In addition, psychophysical experiments for social-touch gestures were carried out in 16 healthy participants. All participants provided informed consent in writing before the start of the experiment. The study was approved by the ethics committees of Linköping University (Dnr 2017/485-31) and complied with the revised Declaration of Helsinki. The participants were seated in a comfortable chair and pillows were provided to ensure minimal discomfort.

Experimenters—standardized touchers. Based on observations of the common physical features of touch communication behavior between people in a close relationship (McIntye et al. unpublished), we developed a set of 'standardized' touch gestures to communicate 'attention', 'happiness', 'calming', 'love', 'gratitude' and 'sadness'. These standardized gestures were applied by trained experimenters to the physiological receptive field of single neurons during microneurography recordings. The experimenter received spoken cues via headphones, first the cue-word, then a countdown (3, 2, 1, go). They were instructed to perform the touch starting from the "go"-signal until they heard a stop signal (3, 2, 1, stop), creating a continuous time window of touch for 10 s. The experimenter was first familiarized with the neuron's receptive field, and was required to touch an area of skin including but not limited to the receptive field. They were also required not to perform any vigorous movements in order to avoid dislodging the recording electrode. Where a single-unit recording was stable enough, data for multiple trial-sets were obtained.

Microneurography. Neural recordings were performed with equipment purpose-built for human microneurography studies from AD Instruments (Oxford, UK; Setup 1) or the Physiology Section, Department of Integrative Medical Biology, Umeå University (Setup 2). The radial neve was visualized using the ultrasound technique (LOGIQ e, GE Healthcare). Then, a high-impedance tungsten recording electrode was inserted percutaneously followed by localization of the nerve by weak electrical stimulation through that electrode (0.02-1 mA, 0.2 ms, 1 Hz; FHC, Inc. Bowdoin, ME, USA). The electrode was insulated, except for the ~5 µm bare tip, with a typical length of 40 mm and shaft diameter of 0.2 mm. In addition to the recording electrode, an indifferent (uninsulated) electrode was inserted subcutaneously, approximately 5 cm away from the nerve. Once the electrode tip was intra-fascicular, minute movements were made to the recording electrode, manually or with a pair of forceps, while stroking the fascicular innervation zone until single-unit activity could be recorded.

After the recording electrode reached a stable position for single-unit recording, each cutaneous afferent (all soft-brush sensitive) was classified by its physiological characteristics, as per the criteria used in Vallbo et al [4]. The mechanical threshold of each cutaneous afferent fibre was determined using Semmes-Weinstein monofilaments (nylon fibre; Aesthesio, Bioseb, Pinellas Park, FL, USA). The monofilaments were applied manually with a rapid onset until the monofilament buckled: If a unit responded to the same (weakest) monofilament in at least 50% of trials, it was taken as the mechanical threshold.

Data analysis for neural recordings: All neural data were recorded and processed using LabChart Pro for Setup 1 (v8.1.5 and PowerLab 16/35 hardware PL3516/P; ADInstruments, Oxford, UK) and SC/ZOOM for Setup 2 (Physiology Section, Department of Integrative Medical Biology, Umeå University). Action potentials were distinguished from background noise with a signal-to-noise ratio of at least 2:1, and were confirmed to have originated from the recorded afferent by a semi-automatic inspection of their morphology.

5 neural parameters were calculated for each social-touch expression: 1) the number of spikes, 2) the peak frequency (inverse of the shortest inter-spike interval), 3) the mean frequency (inverse of the

average inter-spike interval), 4) standard deviation of spike frequency, and 5) the number of "bursts" of firing, defined as the number of inter-spike intervals greater than 1 second.

Motion tracking. We used a custom motion tracking system to quantify the contact in each touch expression, as previously reported [26]. The motion tracking consisted of two main components: a 2-D high definition video camera (HDR-CX625, 9.2 megapixel, Sony Corp., Tokyo, Japan) and a 3-D infrared stereo camera system (Leap Motion, San Francisco, CA). During experiments, while the "toucher" was contacting a participant, the positions of the bones in the toucher's hand were measured in 3-D by the Leap Motion controller at approximately 40-60 Hz, as well as recorded in 2-D high definition video (1280 x 720 pixels) at 30 Hz. The use of both systems together afforded much better results than using either alone.

First, several joints in the fingertip were identified in the video recording by a research assistant—each finger tip, each proximal interphalangeal joint, each metacarpophalangeal joint, and the palm. These joints were tracked in Python using OpenCV-2 CSRT tracking filters. The research assistant observed the accuracy of the tracking filters and reset them to the joint position if they did not align with the video. After this process, an affine camera matrix was fit to translate the 3-D Leap Motion coordinates into the 2-D video coordinates. Several unique hand positions were identified in the Leap Motion recordings and selected for fitting. For each frame of the video, the best-fit unique hand position was translated to the palm coordinates as measured by the Leap Motion, and the optimal rotation was found using an optimization package in Python 2.7 (scipy.optimize). The result was a set of 3-D hand positions, for each frame of the video recording, which generally well-matched the video recording.

After this process, a 30 mm -radius cylindrical plane was fit to the receptive field of the afferent, given time points at which the finger made contact. Contact with this plane was measured using a simple contact model between the Leap Motion hand and this plane. Hand position data from the Leap Motion resulted in 3-D poses, widths, and lengths for each bone in the hand. In custom software, written in Python 2.7, these were translated into cylinders made up of 3-D line segments. Each intersection between these lines segments and the plane representing the receptive field was treated as a contact point.

We examined four quantified touch attributes, which had been considered in prior work [20], [21]. The attributes of 1) contact was determined as a binary value representing whether any bones from the toucher's hand intersected with the receptive field plane 3) Contact area was measured as the area of the convex hull enveloping the contact points for each bone in the hands. 4) Velocity was measured as the mean velocity of the index fingertip.

Statistics. For pairwise comparisons between touch expressions for mean firing rate, ANOVA and post-hoc Tukey's HSD were used to determine significant differences for $p < .05$. Correlations were determined between pleasantness and peak firing rate using a Pearson's R correlation coefficient. Statistics were performed in Python 2.7 using scipy.stats and statsmodels packages.

Machine learning. The five features input to the model were the 5 neural parameters per touch expression (or component gesture): 1) the number of spikes, 2) the peak frequency, 3) the mean frequency, 4) the standard deviation of spike frequency, and 5) the number of "bursts" of spiking (inter-spike intervals > 1 s). A random forest classifier (with default parameters) was used to compare both the touch expression data as well as the component gestures data. Naïve Bayes classifiers and K-NN classifiers were also used with very similar results, but the Random Forest is shown to give the highest classification accuracy. For the touch expression data, a 5-fold cross-valdiation procedure was performed. For the component gestures data, a 10-fold cross-validation procedure was done. All machine learning analysis was performed in Python 2.7 using the scikit-learn packages.

Psychophysics. Pleasantness of each gesture was assessed in a separate experiment with 10 participants. The gestures were presented for a 10-second duration from a trained toucher, delivering nearly identical touches to those in the microneurography experiments. Participants were asked to rate each touch on a visual-analog (VAS) scale of -10 to 10, from “most unpleasant” touch to “most pleasant” touch. Among all participants, each cue was presented 16 or 17 times in total.

Overall conclusions and future work

In this dissertation, we performed significant groundwork towards understanding human-to-human social and emotional touch. The overall goal was to move from a qualitative observation of social touch gestures to a quantified effort with measurements of physical parameters, along with proposed mechanisms of how touch expressions might be encoded in the periphery. First, we observed and quantified how six touch expressions were performed in close adult relationships, noting varying strategies with different recognition rates. Next, we worked towards developing tracking methods to measure contact during microneurography experiments, noting some immediate differences between responses of a C-tactile afferent and a Pacinian (FA-II) afferent. Finally, in a combination microneurography and tracking effort, we identified the roles of key afferents in encoding gestures at the single-unit level, finding some subsets of afferents to be particularly effective at recognizing different human touches, even to the level of differentiation within a single first-order unit.

Our quantitative study of social touch resulted in the optical tracking system, which we found to be very useful given some other preliminary results. When Tegaderm (an extremely thin plastic bandage) was applied to the arm, we found in unpublished studies that firing rates of the C-tactile afferents and HFAs were severely attenuated. Thus, any barrier between direct skin-to-skin contact may have a very significant effect on the measured responses, as well as the emotional and social content. The system also gave us specifications for contact areas, velocities, and durations of naturalistic touches. This information might be very useful, for example, when designing devices to artificially render social touch expressions for communication.

Our technique of simultaneous microneurography and motion tracking recordings was not used to its full extent in Aim 3, and we believe the technique has significant promise in upcoming studies. For instance, one initial reasoning for the simultaneous tracking was to develop more complex transduction functions for each afferent type. Traditional characterization only varies one factor at a time, making a modeling effort for human touch, which co-varies many factors, very difficult. Instead, with early data we were able to fit probability functions to spiking rates when confronted with multivariate stimuli. The early data with some of these fits is shown in Figure 4.1.

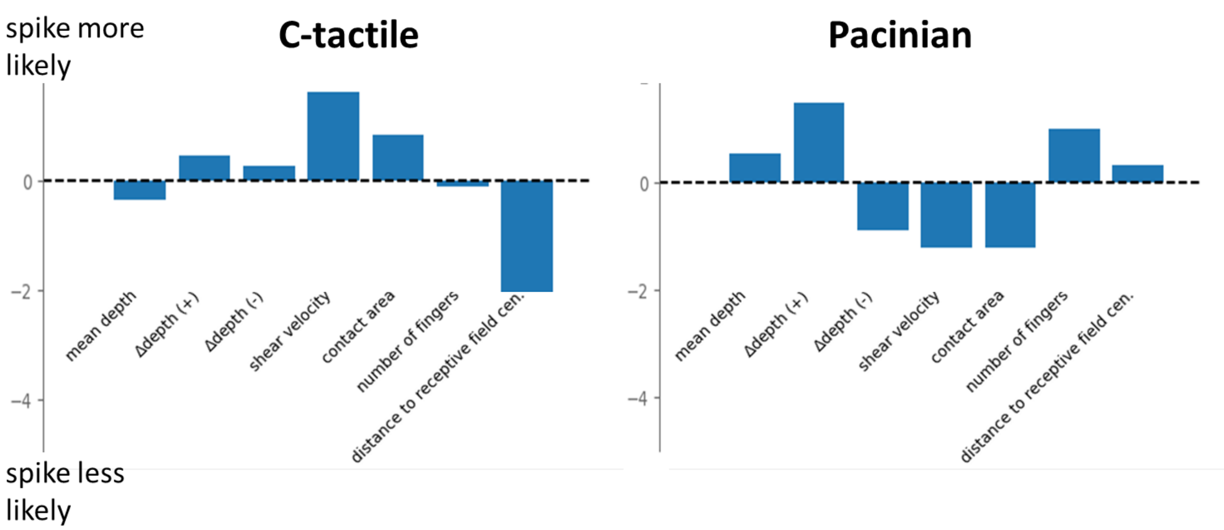

Figure 4.1) Probability coefficients for logistic regression on physical parameters to spiking probability in 10-millisecond bins. We found the C-tactile afferent (left) to have increased probability of response with high shear velocity, and stimulation closer to the receptive field center. We found the Pacinian (FA-II) afferent to have increased response probability with changes in depth.

It was very surprising to find that a single unit first-order unit could be capable of differentiating the gesture. When we originally set out to investigate this question, we were not expecting to find *any* subtypes capable of this feat—for instance, many of the gestures were spread out across the arm significantly, meaning that only part of the gesture was directly on top of the afferent's receptive field. We believe that the single-unit responses may be perceptually important due to some yet unpublished work conducted at Linköping University. They used anesthetic cream (lidocaine) to numb the arm and attenuate/prevent the responses of cutaneous nerves in the arm, and then attempted to see if the touch gestures could still be differentiated. Quite surprisingly, the touches were found to still be discriminable, even though the patient could not see the gestures, and presumably had greatly attenuated tactile sensation. However, considering now that even a single SA-II or HFA may be capable of differentiation, it may be possible that this attenuated response is still enough to identify the gestures.

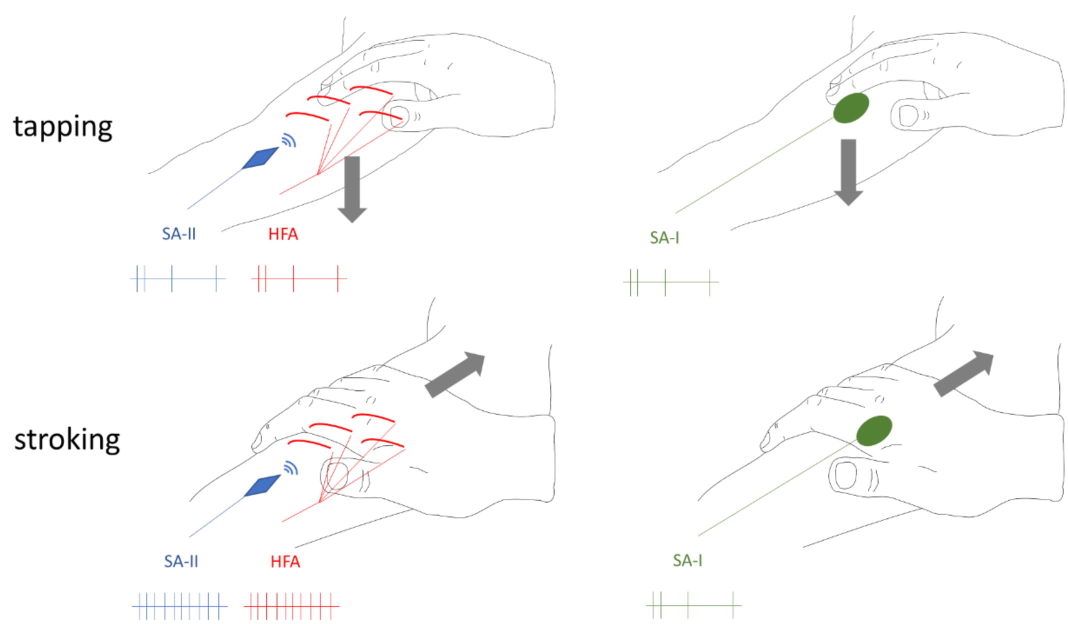

Figure 4.2) Large receptive area of HFA and SA-II, along with their sensitivity to shear, makes their responses differentiable. The SA-I, in contrast, responds just when the receptive field is crossed, and does not reliability respond for each tap, making its responses similar for stroking and tapping.

Future Directions. A proposed effort is to begin investigating the role of the tactile afferent subtypes at the population level. Although it is possible that social touch is differentiable by a single receptor at a time, it seems more likely that thousands of afferents in the forearm may respond at once. Various statistical and machine learning analyses may allow us to predict the output of many neurons, and determine which afferents might be most important at that level.

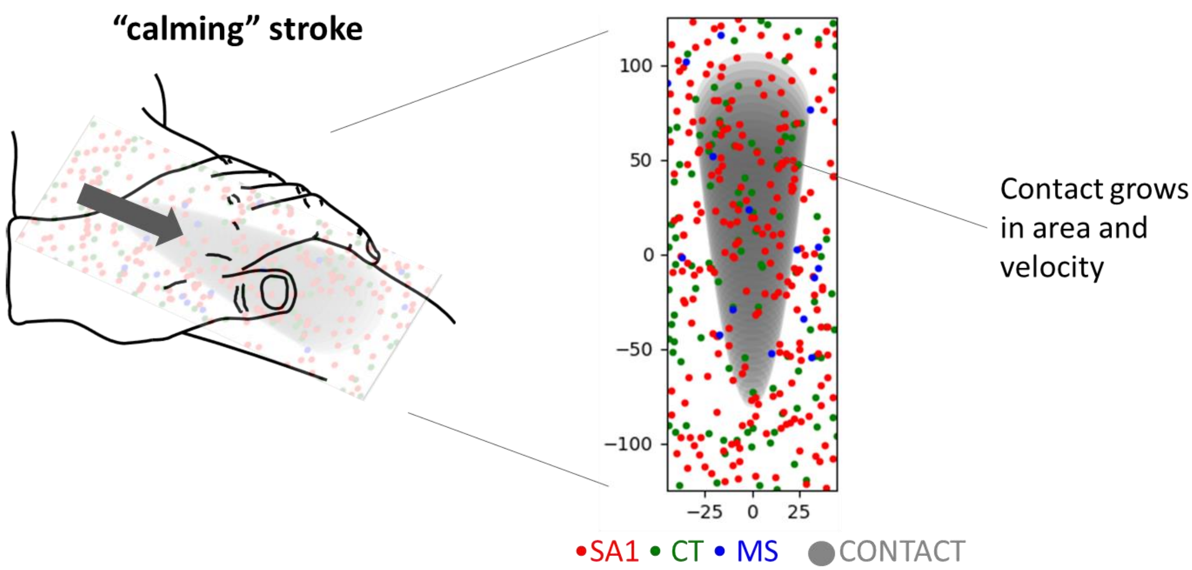

Figure 4.3 A population model of SA-I, C-tactile, and muscle spindle afferents in the forearm for a "calming" stroke. The linear model consists of thousands of afferents, with only 1% shown in the diagram.

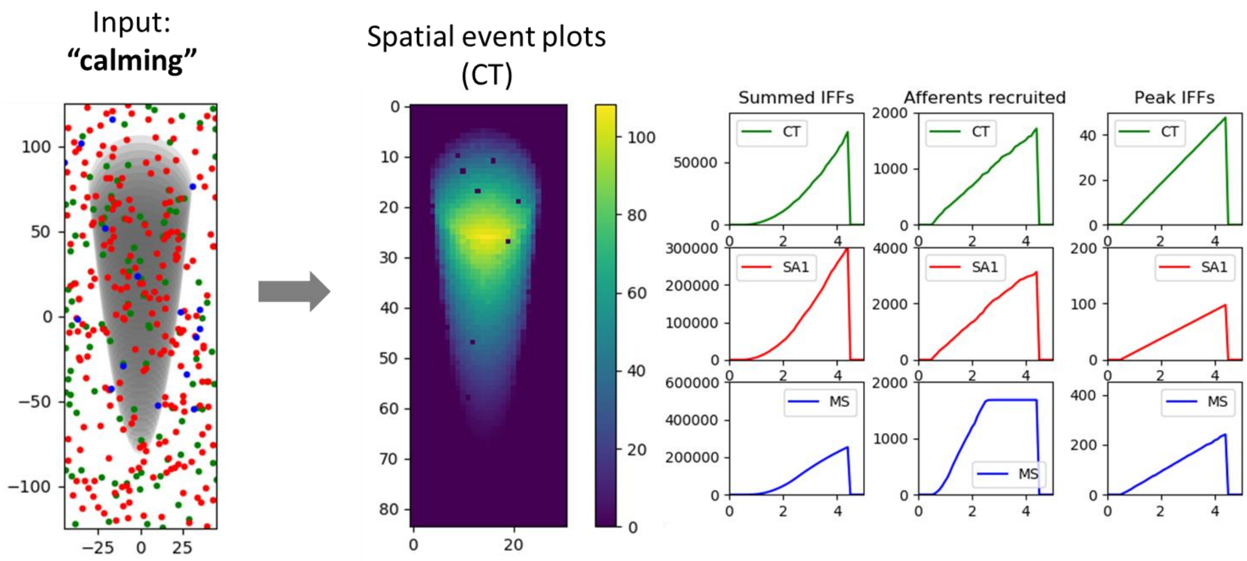

Figure 4.4 A population response to "calming". With spatial event plots (middle) and temporal firing characteristics at the population level (right). Metrics include summed instantaneous firing frequency, the number of afferents recruited, and the peak firing frequency.

Further exploration of the population-level encoding would likely require a modeling effort, which we have made some progress with. The proposed methodology is to use a computational neural model of the forearm as a test-bed for investigating encoding mechanisms (as in Figure 4.3 and 4.4), and then validate these mechanisms via psychophysical experiments using simple 3-D printed devices and "expert touchers" at Linköping University. First, to investigate perception-level encoding, we propose to build a population model of the sensory afferents in the forearm consisting of a few thousand afferents. The input to this model will be the measured contact primitives from human touch, as well as some mechanically measured quantities investigated in Aim 2 such as shear forces and vibration frequency. The output of the model will include spatial firing patterns such as gradient sum and receptor recruitment as well as temporal firing patterns such as peak and mean firing rates within each receptor subtype. We plan to use gestures measured from Aim 1 as inputs to the model, and perform both machine learning analysis such as logistic regression as well as traditional statistical and clustering analysis to determine codes in the neural output that best differentiate or represent each gesture. Once coming up with candidate encoding mechanisms, we plan to again use our model to design physical contact inputs that efficiently evoke them. Finally, we validate the mechanisms by recreating the physical contact inputs from the modeling in human-subjects psychophysical experiments, by employing both 1) simple 3-D printed devices, which might limit the contact area or vibrate etc., and 2) “expert touchers” at Linköping University, who will perform gestures closely to our designated input (as verified by the motion tracking system).

Contributions

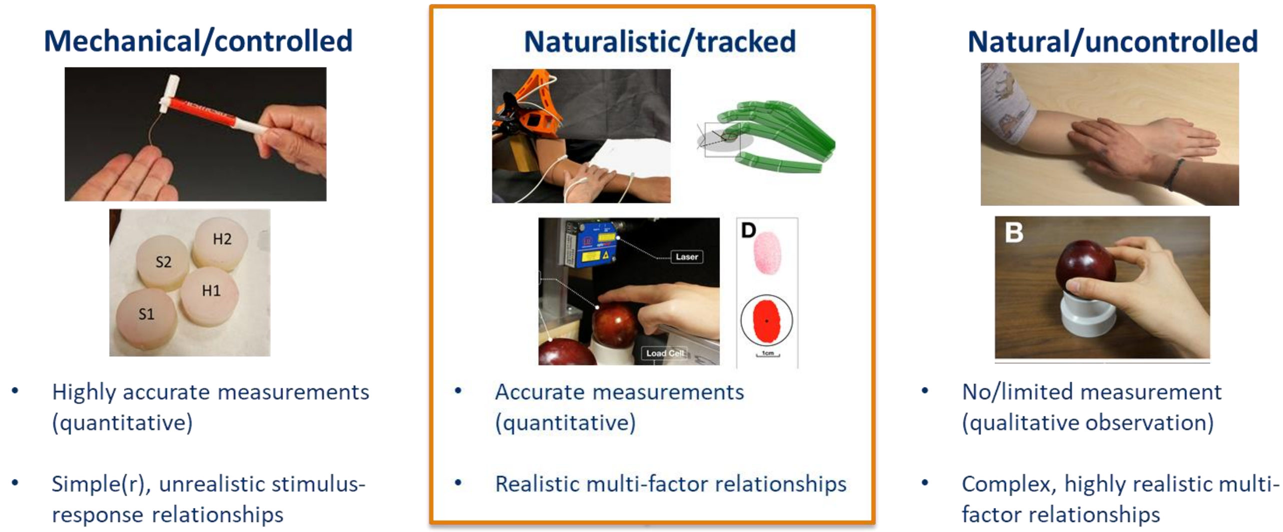

C.1 Diagram of my niche in naturalistic/tracked experiments.

Overall, I believe that the main contribution of this dissertation is in combining the quantitative measurements characteristic of traditional, controlled experiments with the study of naturalistic interactions. By utilizing many disciplines of engineering to rapidly develop highly specialized tools, we are able to use tracking to measure specific quantities of interest during naturalistic experiments. The tactile system in particular is well suited for this kind of study, as perceptual cues (contact area, force etc.) are as much a function of the stimulus as they are a function of how the stimulus is explored. This means that study in a natural context is vital towards expanding our understanding of touch perception.

This approach has allowed us to measure skin-to-skin interactions between humans, and finger pad contact with natural materials such as fruit. We have seen that certain cues, when used in a natural setting, are more effective or efficient than others. We have also been able to examine peripheral nerve responses to their actual stimuli of interest, the touch of another human. In future work, we hope that this type of study will continue to get the "best of both worlds" of quantified, natural interaction.

Methodological Contributions

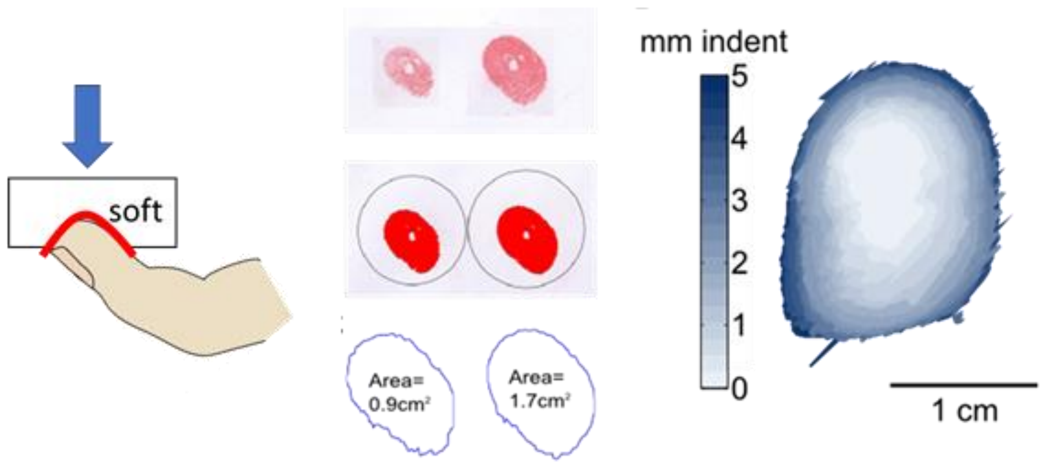

C.2 Ink-based method to measure contact area [23], [24], [50].

With this methodology, the contact area between the finger pad an any type of object can be measured, at a peak displacement into the substrate. We initially used this method to simply measure the shape of the contact area during an indentation, as many haptic displays in the past had modeled the contact area as a simple circle, while the actual shape is more complicated and elliptical. Later, the technique proved useful for measuring contact area with curved silicone elastomers of differing radii of curvature, and even with soft fruits (plums). The method is very flexible and easy to analyze with simple images.

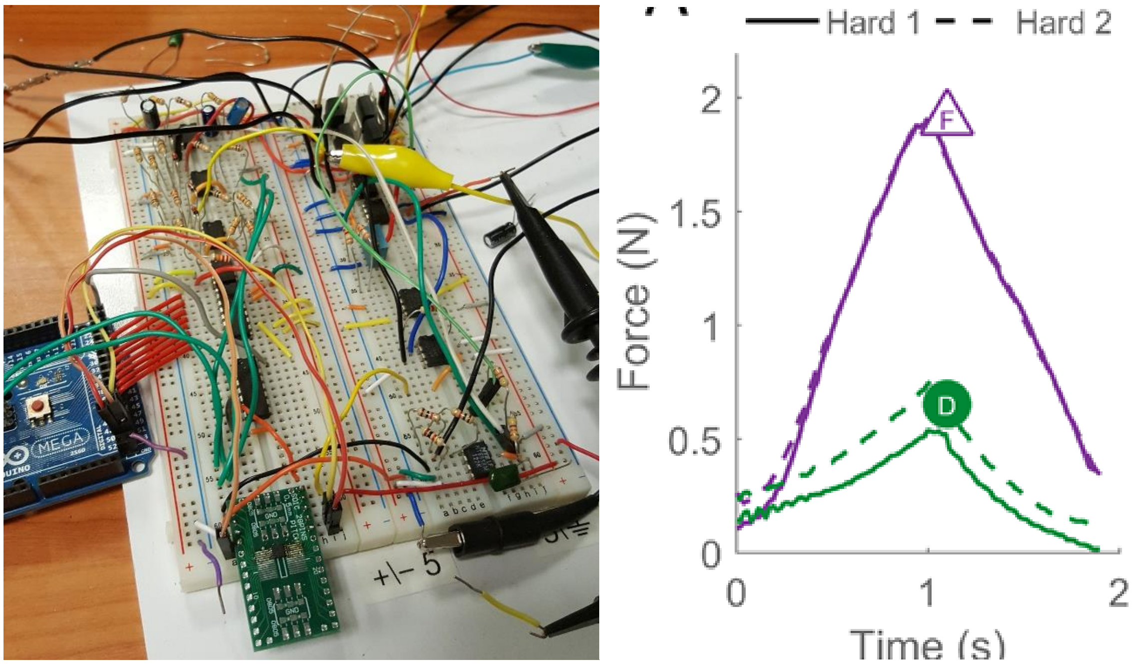

C.3 Force-control circuitry for nonlinear elastic interactions between finger pad and compliant stimulus [23], [50].

I designed a system to control force over time as an elastic stimulus is pressed into the finger pad at varying rates. It is effective for stimuli of moduli from 20 to 200 kPa, at rates of about 0.5 N/s to 3 N/s. Indenting into the finger pad is tricky because the finger itself is highly nonlinear in stiffness. That is, when pressing into the finger at low displacement, the stimulus needs to make large movements to increase force---when pressing deep into the finger, however, the stimulus needs to make only very small movements. The problem is complicated further in psychophysical experiments, where stimuli of varying elasticities need to be changed out quickly without changing the setup. The general principle of this circuitry was to measure the force rate (via differentiation of the load cell voltage) and the current velocity (from the motion controller). A division is performed by a microcontroller which scales the error signal by the instantaneous stiffness (df/dt divided by dx/dt).

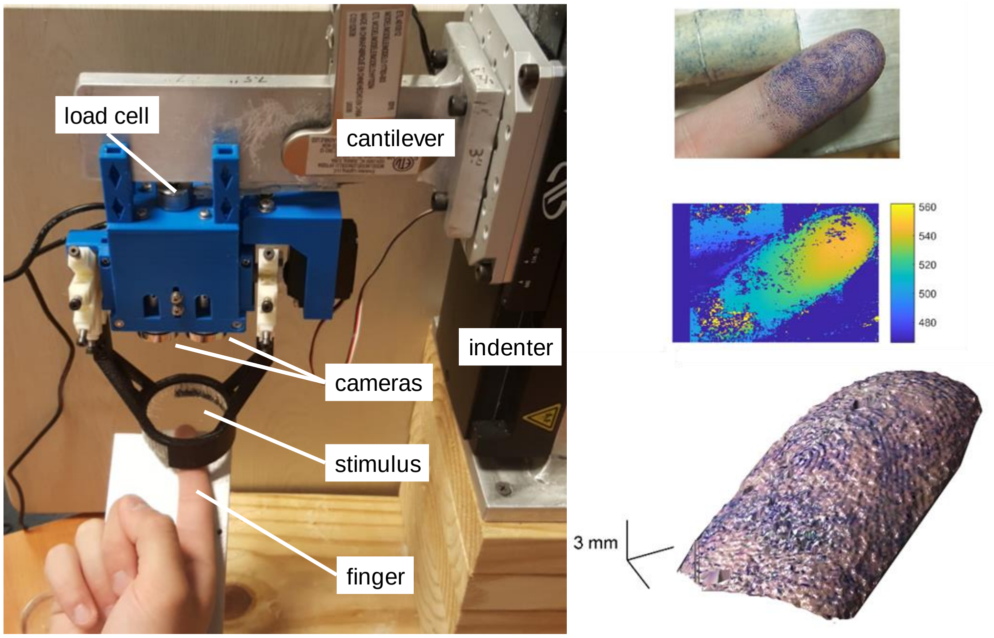

C.4 Stereo imaging technique to measure 3-d deformation of the finger pad surface [51].

Although the prior methods to measure contact area were effective for a first look, and were very portable to many substrates, we lacked continuous measurement over time, or 3-D spatial detail about how the finger pad deforms. With a stereo imaging system, we were able to measure how the finger pad changes shape when pressed into transparent silicone elastomers. This process required marking of the finger pad with ink in a speckle pattern, and corrections to account for the refraction of light through the silicone. Further techniques with the system seek to simplify and smooth the contact region via elliptical fitting of the 3-D surface.

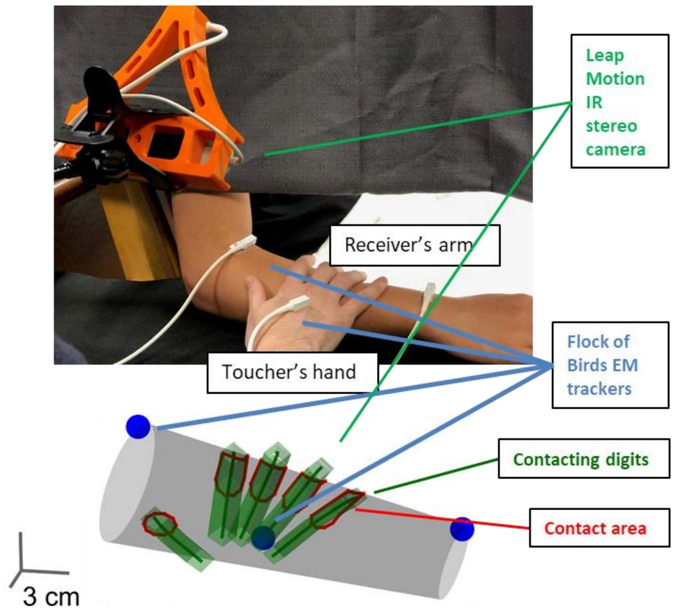

C.5 Optical and electromagnetic measurement system to quantify skin-to-skin contact in human-to-human touch [36].

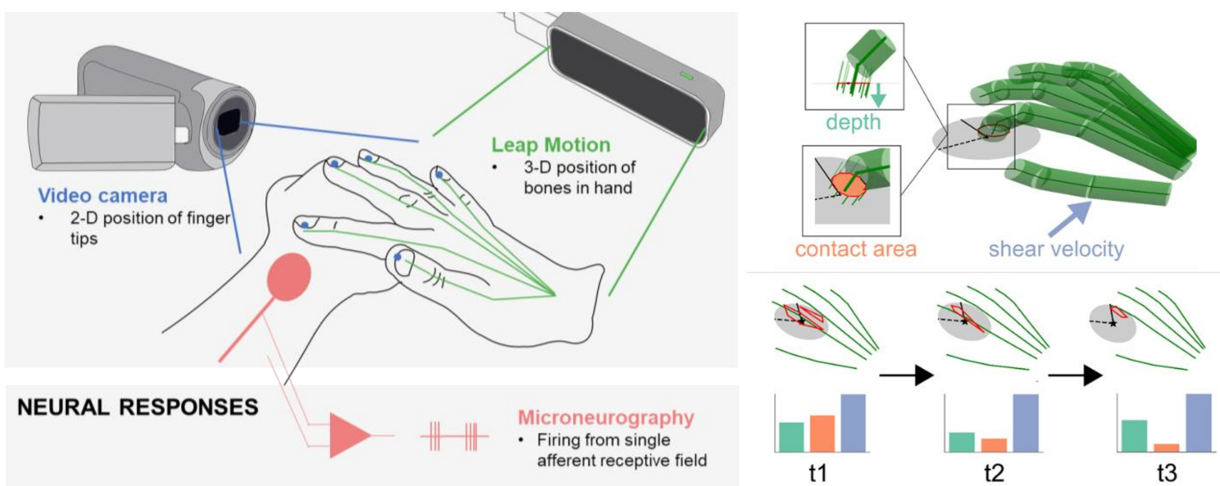

C.6 Optical system for simultaneous measurement of neural responses and skin-to-skin contact [26].

These systems combined optical measurement with electromagnetic tracking. In software, a very simple contact model of intersecting 3-D rays was used to estimate hand-to-arm contact between two people. The system is novel in that no kind of sensor mat or pad separates the two people, allowing for naturalistic contact and touch communication.

Main Scientific Contributions

- Force-area relationships between the index finger and soft, cylindrical stimuli are similar between people when the approach angle is consistent. [24]
- In passive touch, force-rate cues are more effective than displacement-rate cues for differentiating stiff elastic stimuli, and can be utilized efficiently at lower displacement and force levels. [23]
- By indenting less compliant material into the finger pad at a lower force-rate than a more compliant material, participants can be confused as to which object is softer. [23]
- The finger pad changes shape (flattens) significantly more when pressing into hard objects as compared to soft objects. [51]
- When pressing into objects harder than the finger pad, the finger first flattens out before eventually penetrating into the material. This does not occur for softer materials. [in progress]
- Humans use 2-5 expression strategies to communicate a set of 6 emotive words, with varying velocities, touch durations, and contact areas. [36]
- Some emotive words such as “attention” are immediately recognized through touch, even with significant variability in how the gesture was performed. [36]
- C-tactile afferents respond well during human-to-human stroking, while Pacinian afferents respond in time with tapping gestures. [26]
- A single afferent of two types (Hair follicle or SA-II afferent) may be capable of discerning a set of emotive touch gestures, suggesting the circuitry exists to discriminate social touches very distally in the periphery. [in progress]

Publications

Accepted works

Journal Papers

1. Boehme, R., **Hauser, S.C.**, Gerling, G.J., Heilig, M., & Olausson, H. (2019). Distinction of self-produced touch and social touch at cortical and spinal cord levels. Proceedings of the National Academy of Sciences, 116(6), 2290-2299.
2. Gerling, G.J., **Hauser, S.C.**, Soltis, B.R., Bowen, A.K., Fanta, K.D., & Wang, Y. (2018). A Standard Methodology to Characterize the Intrinsic Material Properties of Compliant Test Stimuli. IEEE transactions on haptics, 11(4), 498-508.
3. **Hauser, S.C.**, & Gerling, G.J. (2017). Force-rate cues reduce object deformation necessary to discriminate compliances harder than the skin. IEEE transactions on haptics, 11(2), 232-240.

Conference Papers (Peer-reviewed publications)

1. **Hauser, S.C.,** McIntyre, S., Israr, A., Olausson, H., and Gerling, G.J., (2019, July) Uncovering Human-to-Human Physical Interactions that Underlie Emotional and Affective Touch Communication. In World Haptics Conference (pp.407-413), 2019
2. **Hauser, S.C.,** Nagi, S.S., McIntyre, S., Israr, A., Olausson, H., and Gerling, G.J., (2019, July) From Human-to-Human Touch to Peripheral Nerve Responses. In World Haptics Conference (pp. 592-598), 2019

3. Xu, C., **Hauser, S.C.,** Wang, Y., and Gerling, G.J., (2019, Julys) Roles of Force Cues and Proprioceptive Joint Angles in Active Exploration of Compliant Objects. In World Haptics Conference (pp. 353-359), 2019
4. Xu, C., Wang, Y., **Hauser, S. C.**, & Gerling, G. J. (2018, September). In the Tactile Discrimination of Compliance, Perceptual Cues in Addition to Contact Area Are Required. In Proceedings of the Human Factors and Ergonomics Society Annual Meeting (Vol. 62, No. 1, pp. 1535-1539). Sage CA: Los Angeles, CA: SAGE Publications.
5. **Hauser, S. C.**, & Gerling, G. J. (2018, March). Imaging the 3-D deformation of the finger pad when interacting with compliant materials. In 2018 IEEE Haptics Symposium (HAPTICS) (pp. 7-13). IEEE.
6. **Hauser, S. C.**, & Gerling, G. J. (2016, April). Measuring tactile cues at the fingerpad for object compliances harder and softer than the skin. In 2016 IEEE Haptics Symposium (HAPTICS) (pp. 247-252). IEEE

W.I.P. (short) Conference Papers

1. Xu, C., He, H., **Hauser, S.C.**, and Gerling, G.J., "Measurement of Touch Interaction Cues in Discriminating Soft Fruit," for poster presentation at *World Haptics Conference (WHC),* 2019
2. **Hauser, S.C.,** McIntyre, S., Olausson, H., and Gerling, G.J., "Quantifying physical contact underlying affective touch," for poster presentation at *Eurohaptics*, 2018
3. Sharpe, A.R., **Hauser, S.C.**, and Gerling, G.J. "A multi-chamber pneumatic actuator to render a percept of softness to the finger pad," for poster presentation at *IEEE Haptics Symposium (HAPTICS),* 2018
4. **Hauser, S.C.** and Gerling, G.J., "Imaging the finger pad surface while deforming compliant materials," for poster presentation at *World Haptics Conference*, 2017

In progress works

Journal Papers

1. **Hauser, S.C. †,**, Nagi, S.S. †, McIntyre, S., Jarocka, E., Israr, A., Olausson, H. and Gerling, G.J., "Social touch gestures can be differentiated by single first-order tactile afferents"
2. McIntyre, S., Boehme, R., **Hauser, S.C.**, Kusztor, A., Mongou, A., Novembre, G., Gerling, G.J., Isager, P.M., Israr, A., Nagi, S.S., Abnousi, F., Lumpkin, E.A., Bjornsdotter, M., Olausson, H., "Tactile emojis and the language of social touch"

References

[1] M. J. Hertenstein, D. Keltner, B. App, B. A. Bulleit, and A. R. Jaskolka, “Touch communicates distinct emotions.,” *Emotion*, vol. 6, no. 3, p. 528, 2006.

[2] M. J. Hertenstein, R. Holmes, M. McCullough, and D. Keltner, “The communication of emotion via touch.,” *Emotion*, vol. 9, no. 4, p. 566, 2009.

[3] J. T. Suvilehto, E. Glerean, R. I. Dunbar, R. Hari, and L. Nummenmaa, “Topography of social touching depends on emotional bonds between humans,” *Proceedings of the National Academy of Sciences*, vol. 112, no. 45, pp. 13811–13816, 2015.

[4] A. B. Vallbo and K. E. Hagbarth, “Activity from skin mechanoreceptors recorded percutaneously in awake human subjects,” *Exp. Neurol.*, vol. 21, no. 3, pp. 270–289, Jul. 1968.

[5] Å. Vallbo, H. Olausson, and J. Wessberg, “Unmyelinated afferents constitute a second system coding tactile stimuli of the human hairy skin,” *Journal of neurophysiology*, vol. 81, no. 6, pp. 2753–2763, 1999.

[6] H. Olausson *et al.*, “Unmyelinated tactile afferents signal touch and project to insular cortex,” *Nature neuroscience*, vol. 5, no. 9, p. 900, 2002.

[7] R. Ackerley, H. B. Wasling, J. Liljencrantz, H. Olausson, R. D. Johnson, and J. Wessberg, “Human C-tactile afferents are tuned to the temperature of a skin-stroking caress,” *Journal of Neuroscience*, vol. 34, no. 8, pp. 2879–2883, 2014.

[8] L. S. Löken, J. Wessberg, F. McGlone, and H. Olausson, “Coding of pleasant touch by unmyelinated afferents in humans,” *Nature neuroscience*, vol. 12, no. 5, p. 547, 2009.

[9] H. Culbertson, C. M. Nunez, A. Israr, F. Lau, F. Abnousi, and A. M. Okamura, “A social haptic device to create continuous lateral motion using sequential normal indentation,” presented at the Haptics Symposium (HAPTICS), 2018 IEEE, 2018, pp. 32–39.

[10] S.-H. Woo *et al.*, “Piezo2 is required for Merkel-cell mechanotransduction,” *Nature*, vol. 509, no. 7502, p. 622, 2014.

[11] M. M. Jung, X. L. Cang, M. Poel, and K. E. MacLean, “Touch challenge’15: Recognizing social touch gestures,” presented at the Proceedings of the 2015 ACM on International Conference on Multimodal Interaction, 2015, pp. 387–390.

[12] M. D. Cooney, S. Nishio, and H. Ishiguro, “Recognizing affection for a touch-based interaction with a humanoid robot,” presented at the Intelligent Robots and Systems (IROS), 2012 IEEE/RSJ International Conference on, 2012, pp. 1420–1427.

[13] J. Chang, K. MacLean, and S. Yohanan, “Gesture recognition in the haptic creature,” presented at the International Conference on Human Haptic Sensing and Touch Enabled Computer Applications, 2010, pp. 385–391.

[14] A. Flagg and K. MacLean, “Affective touch gesture recognition for a furry zoomorphic machine,” presented at the Proceedings of the 7th International Conference on Tangible, Embedded and Embodied Interaction, 2013, pp. 25–32.

[15] K. Altun and K. E. MacLean, “Recognizing affect in human touch of a robot,” *Pattern Recognition Letters*, vol. 66, pp. 31–40, 2015.

[16] R. I. Dunbar, “The social role of touch in humans and primates: behavioural function and neurobiological mechanisms,” *Neuroscience & Biobehavioral Reviews*, vol. 34, no. 2, pp. 260–268, 2010.

[17] F. McGlone, J. Wessberg, and H. Olausson, “Discriminative and affective touch: sensing and feeling,” *Neuron*, vol. 82, no. 4, pp. 737–755, 2014.

[18] I. Morrison *et al.*, “Reduced C-afferent fibre density affects perceived pleasantness and empathy for touch,” *Brain*, vol. 134, no. 4, pp. 1116–1126, 2011.

[19] V. Gazzola, M. L. Spezio, J. A. Etzel, F. Castelli, R. Adolphs, and C. Keysers, “Primary somatosensory cortex discriminates affective significance in social touch,” *Proceedings of the National Academy of Sciences*, vol. 109, no. 25, pp. E1657–E1666, 2012.

[20] A. Israr and F. Abnousi, “Towards Pleasant Touch: Vibrotactile Grids for Social Touch Interactions,” presented at the Extended Abstracts of the 2018 CHI Conference on Human Factors in Computing Systems, 2018, p. LBW131.

[21] B. B. Edin, G. K. Essick, M. Trulsson, and K. A. Olsson, “Receptor encoding of moving tactile stimuli in humans. I. Temporal pattern of discharge of individual low-threshold mechanoreceptors,” *Journal of Neuroscience*, vol. 15, no. 1, pp. 830–847, 1995.

[22] K. O. Johnson, T. Yoshioka, and F. Vega–Bermudez, “Tactile functions of mechanoreceptive afferents innervating the hand,” *Journal of Clinical Neurophysiology*, vol. 17, no. 6, pp. 539–558, 2000.

[23] S. C. Hauser and G. J. Gerling, “Force-rate cues reduce object deformation necessary to discriminate compliances harder than the skin,” *IEEE Transactions on Haptics*, vol. 11, no. 2, pp. 232–240, 2018.

[24] S. C. Hauser and G. J. Gerling, “Measuring tactile cues at the fingerpad for object compliances harder and softer than the skin,” presented at the IEEE Haptics Symposium:[proceedings]. IEEE Haptics Symposium, 2016, vol. 2016, p. 247.

[25] J. Guna, G. Jakus, M. Pogačnik, S. Tomažič, and J. Sodnik, “An analysis of the precision and reliability of the leap motion sensor and its suitability for static and dynamic tracking,” *Sensors*, vol. 14, no. 2, pp. 3702–3720, 2014.

[26] S. C. Hauser, S. S. Nagi, S. McIntyre, A. Israr, H. Olausson, and G. J. Gerling, “From Human-to-Human Touch to Peripheral Nerve Responses,” presented at the World Haptics Conference 2019, 2019, p. in press.

[27] J. Wessberg and U. Norrsell, “A system of unmyelinated afferents for innocuous mechanoreception in the human skin,” *Brain research*, vol. 628, no. 1–2, pp. 301–304, 1993.

[28] A. Vallbo and R. S. Johansson, “Properties of cutaneous mechanoreceptors in the human hand related to touch sensation,” *Hum Neurobiol*, vol. 3, no. 1, pp. 3–14, 1984.

[29] R. S. Johansson, U. Landstrom, and R. Lundstrom, “Responses of mechanoreceptive afferent units in the glabrous skin of the human hand to sinusoidal skin displacements,” *Brain Res*, vol. 244, no. 1, pp. 17–25, 1982.

[30] A. I. Weber *et al.*, “Spatial and temporal codes mediate the tactile perception of natural textures,” *Proceedings of the National Academy of Sciences*, p. 201305509, 2013.

[31] I. Nelken, Y. Rotman, and O. B. Yosef, “Responses of auditory-cortex neurons to structural features of natural sounds,” *Nature*, vol. 397, no. 6715, p. 154, 1999.

[32] Y. Dan, J. J. Atick, and R. C. Reid, “Efficient coding of natural scenes in the lateral geniculate nucleus: experimental test of a computational theory,” *Journal of Neuroscience*, vol. 16, no. 10, pp. 3351–3362, 1996.

[33] N. Kanwisher, J. McDermott, and M. M. Chun, “The Fusiform Face Area: A Module in Human Extrastriate Cortex Specialized for Face Perception,” *J. Neurosci.*, vol. 17, no. 11, p. 4302, Jun. 1997.

[34] P. Belin, R. J. Zatorre, P. Lafaille, P. Ahad, and B. Pike, “Voice-selective areas in human auditory cortex,” *Nature*, vol. 403, p. 309, Jan. 2000.

[35] R. Boehme, S. Hauser, G. J. Gerling, M. Heilig, and H. Olausson, “Distinction of self-produced touch and social touch at cortical and spinal cord levels,” *Proc Natl Acad Sci USA*, p. 201816278, Jan. 2019.

[36] S. Hauser, S. McIntyre, A. Israr, H. Olausson, and G. Gerling, “Uncovering Human-to-Human Physical Interactions that Underlie Emotional and Affective Touch Communication,” presented at the World Haptics Conference, 2019, p. in press.
[37] J. K. Shoemaker, S. A. Klassen, M. B. Badrov, and P. J. Fadel, “Fifty years of microneurography: learning the language of the peripheral sympathetic nervous system in humans,” *Journal of neurophysiology*, vol. 119, no. 5, pp. 1731–1744, 2018.
[38] A. B. Vallbo, H. Olausson, J. Wessberg, and N. Kakuda, “Receptive field characteristics of tactile units with myelinated afferents in hairy skin of human subjects,” *J. Physiol. (Lond.)*, vol. 483 (Pt 3), pp. 783–795, Mar. 1995.
[39] B. B. Edin, P. A. Bäckström, and L. O. Bäckström, “Single unit retrieval in microneurography: a microprocessor-based device controlled by an operator,” *J. Neurosci. Methods*, vol. 24, no. 2, pp. 137–144, Jun. 1988.
[40] S. McIntyre *et al.*, “Affective touch communication in close adult relationships,” *arXiv preprint arXiv:1905.02613*, 2019.
[41] M. J. Hertenstein, J. M. Verkamp, A. M. Kerestes, and R. M. Holmes, “The communicative functions of touch in humans, nonhuman primates, and rats: A review and synthesis of the empirical research,” *Genetic, Social, and General Psychology Monographs*, vol. 132, no. 1, pp. 5–94, 2007.
[42] G. Macefield, S. Gandevia, and D. Burke, “Perceptual responses to microstimulation of single afferents innervating joints, muscles and skin of the human hand.,” *The Journal of Physiology*, vol. 429, no. 1, pp. 113–129, 1990.
[43] J. Ochoa and E. Torebjörk, “Sensations evoked by intraneural microstimulation of single mechanoreceptor units innervating the human hand.,” *The Journal of physiology*, vol. 342, no. 1, pp. 633–654, 1983.
[44] J. Liljencrantz and H. Olausson, “Tactile C fibers and their contributions to pleasant sensations and to tactile allodynia,” *Frontiers in behavioral neuroscience*, vol. 8, p. 37, 2014.
[45] I. Croy, A. Luong, C. Triscoli, E. Hofmann, H. Olausson, and U. Sailer, “Interpersonal stroking touch is targeted to C tactile afferent activation,” *Behavioural Brain Research SreeTestContent1*, vol. 297, pp. 37–40, 2016.
[46] R. Johansson, U. Landstro, and R. Lundstro, “Sensitivity to edges of mechanoreceptive afferent units innervating the glabrous skin of the human hand,” *Brain research*, vol. 244, no. 1, pp. 27–32, 1982.
[47] R. Johansson and Å. Vallbo, “Spatial properties of the population of mechanoreceptive units in the glabrous skin of the human hand,” *Brain research*, vol. 184, no. 2, pp. 353–366, 1980.
[48] S. Mohammad, “Obtaining reliable human ratings of valence, arousal, and dominance for 20,000 English words,” presented at the Proceedings of the 56th Annual Meeting of the Association for Computational Linguistics (Volume 1: Long Papers), 2018, pp. 174–184.
[49] J. A. Russell and A. Mehrabian, “Evidence for a three-factor theory of emotions,” *Journal of research in Personality*, vol. 11, no. 3, pp. 273–294, 1977.
[50] C. Xu, Y. Wang, S. C. Hauser, and G. J. Gerling, “In the Tactile Discrimination of Compliance, Perceptual Cues in Addition to Contact Area Are Required,” in *Human Factors and Ergonomics Society 2018*, 2018.
[51] S. C. Hauser and G. J. Gerling, “Imaging the 3-D deformation of the finger pad when interacting with compliant materials,” presented at the Haptics Symposium (HAPTICS), 2018 IEEE, 2018, pp. 7–13.